1 Phenylacetyl-CoA, not phenylacetic acid, attenuates CepIR-regulated virulence in *Burkholderia*
2 *cenocepacia*
3
4 Tasia Joy Lightly[a], Kara L. Frejuk[a], Marie-Christine Groleau[c], Laurent R. Chiarelli[d], Cor Ras[e],
5 Silvia Buroni[d], Eric Déziel[c], John L. Sorensen[f] and Silvia T. Cardona[a,b#]
6
7 [a]Department of Microbiology, University of Manitoba, Winnipeg, Canada
8 [b]Department of Medical Microbiology & Infectious Diseases, University of Manitoba,
9 Winnipeg, Canada
10 [c]Armand-Frappier Santé Biotechnologie Center, Institut National de la Recherche Scientifique
11 (INRS), Laval, Canada
12 [d]Department of Biology and Biotechnology "Lazzaro Spallanzani", University of Pavia, Pavia,
13 Italy
14 [e]Department of Biotechnology, Delft University of Technology, Delft, The Netherlands
15 [f]Department of Chemistry, University of Manitoba, Winnipeg, Canada
16
17 Running Head: Phenylacetyl-CoA inhibits LuxIR-type quorum sensing
18
19 #Address correspondence to Silvia T. Cardona, Silvia.Cardona@umanitoba.ca
20
21 Abstract word count: 206
22 Importance word count: 149
23 Text word count: 4,224

Abstract

During phenylalanine catabolism, phenylacetic acid (PAA) is converted to phenylacetyl-CoA (PAA-CoA) by a ligase, PaaK, and then epoxidized by a multicomponent monooxygenase, PaaABCDE, before further degradation to the TCA cycle. In the opportunistic pathogen *Burkholderia cenocepacia,* loss of *paaABCDE* attenuates virulence factor expression, which is under control of the LuxIR-like quorum sensing system, CepIR. To further investigate the link between CepIR-regulated virulence and PAA catabolism, we created knockout mutants of the first step of the pathway (PAA-CoA synthesis by PaaK) and characterized them in comparison to a *paaABCDE* mutant using liquid chromatography/mass spectrometry (LC-MS/MS) and virulence assays. We found that while loss of PaaABCDE decreased virulence, deletion of the *paaK* genes resulted in a more virulent phenotype than the wild type strain. Deletion of either *paaK* or *paaABCDE* led to higher levels of released PAA but no differences in internal accumulation, compared to wild type. While we found no evidence of direct *cepIR* downregulation by PAA-CoA or PAA, a low virulence *cepR* mutant reverted to a virulent phenotype upon removal of the *paaK* genes. On the other hand, removal of *paaABCDE* in the *cepR* mutant did not impact its attenuated phenotype. Together, our results suggest an indirect role for PAA-CoA in supressing *B. cenocepacia* CepIR-activated virulence.

Importance

The opportunistic pathogen *Burkholderia cenocepacia* uses a chemical signal process called quorum sensing (QS) to produce virulence factors. In *B. cenocepacia*, QS relies on the presence of the transcriptional regulator CepR, which upon binding QS signal molecules, activates virulence. In this work, we found that even in the absence of CepR, *B. cenocepacia* can elicit a

47 pathogenic response if phenylacetyl-CoA, an intermediate of the phenylacetic acid degradation
48 pathway, is not produced. Instead, accumulation of phenylacetyl-CoA appears to attenuate
49 pathogenicity. Therefore, we have discovered that it is possible to trigger virulence in the
50 absence of CepR, challenging the classical view of activation of virulence by this QS
51 mechanism. Our work provides new insight into the relationship between metabolism and
52 virulence in opportunistic bacteria. We propose that, in the event that QS signaling molecules
53 cannot accumulate to trigger a pathogenic response, a metabolic signal can still activate virulence
54 in *B. cenocepacia*.
55

56 **Introduction**

57 Intercellular communication in bacteria, or quorum sensing (QS), relies on the production
58 and detection of signalling molecules to regulate gene expression in a cell-density dependent
59 manner (1, 2). In many Gram-negative bacteria, LuxI homologs synthesize *N*-acyl homoserine
60 lactones (AHLs) as signalling molecules. These small diffusible molecules accumulate
61 extracellularly as the population increases until the concentration is sufficient for AHLs to return
62 into the cell where they bind LuxR-type transcriptional regulators. Complexing of the AHL to
63 the LuxR homolog results in a conformational change that alters the ability of the transcriptional
64 regulator to bind DNA and regulate gene expression (3). Many of the genes regulated by QS
65 control expression of virulence traits, which are important for bacteria to establish infection (4).
66 A bacterium with a LuxIR-type QS system is *Burkholderia cenocepacia*, a member of the
67 *Burkholderia cepacia* complex (5). The strain *B. cenocepacia* K56-2, isolated from the sputum
68 of a cystic fibrosis patient, has two complete LuxIR-type QS systems, CepIR and CciIR, and one
69 orphan transcriptional regulator, CepR2 (5, 6). The regulons of CepR and CciR have been

70 examined and a large number of the genes that are regulated are linked to virulence (7). While
71 CepR and CciR have separate regulons, certain genes are regulated by both in a reciprocal
72 manner (7). CepR positively regulates gene expression, whereas CciR is responsible for negative
73 gene regulation (7). While these two systems regulate certain genes in a reciprocal manner,
74 rather than hierarchically like those of *Pseudomonas aeruginosa,* the transcription of both *cepI*
75 and *cciIR* is dependent on CepR and in turn CciR negatively regulates the expression of *cepI* (7,
76 8). CepR and CciR both positively regulate their canonical autoinducer synthase and negatively
77 regulate their own transcription (8, 9). CepI mainly produces *N*-octanoyl homoserine lactone
78 (C8-HSL) with slight production of *N*-hexanoyl homoserine lactone (C6-HSL), whereas CciI
79 synthesizes C6-HSL with slight secondary production of C8-HSL (8, 10). CepR2 lacks a cognate
80 AHL synthase and has been shown to regulate known QS-regulated genes independent of a
81 signalling molecule (11).

82 Several lines of evidence point to metabolic adaptation as an important component of
83 virulence regulation (12–15). In this context, high levels of phenylacetic acid (PAA) have been
84 linked to evasion of the immune response by *Acinetobacter* (16), inhibition of pathogenicity of
85 the fungus *Rhizoctonia solani* (17), and downregulation of virulence gene expression in *B.*
86 *cenocepacia* (18). The PAA degradation pathway is a central route by which diverse aromatic
87 compounds, such as phenylalanine, converge and are directed to the tricarboxylic acid (TCA)
88 cycle (19). In *Escherichia coli* K12*,* PAA is converted to phenylacetyl-Coenzyme A (PAA-CoA)
89 by the action of a phenylacetyl-CoA ligase*,* PaaK (19). The conversion to PAA-CoA by PaaK
90 can be reverted to PAA by the action of PaaI, a thioesterase, to prevent accumulation should
91 downstream steps be disrupted (20). Next, PAA-CoA is epoxidized by the multicomponent
92 monooxygenase, PaaABCDE and then further degraded into succinyl-CoA and acetyl-CoA (19).

93 We previously found that CepIR-regulated virulence traits and *cepI* and *cepR* promoter
94 activity were downregulated in a *B. cenocepacia* mutant of the *paaABCDE* operon that released
95 PAA (18). We also demonstrated that PAA could be produced to detectable levels in wild type *B.*
96 *cenocepacia* K56-2 under certain conditions, suggesting a potential physiological role of the
97 regulation of virulence by this molecule (21). However, the PaaABCDE mutant is still able to
98 degrade PAA to PAA-CoA. Therefore, the metabolite responsible and the mechanism of the
99 regulation of virulence by accumulated PAA-metabolites is not known. In this work, we further
100 characterized mutants of the PAA degradation pathway to show that the loss of PaaK function
101 increases virulence, suggesting that PAA-CoA is responsible for the attenuation phenotype.
102 While we found no evidence of a direct effect of PAA-CoA on CepI activity or the formation of
103 CepR:C8-HSL complexes, our results are consistent with a parallel mechanism that uses PAA-
104 CoA, or a derivative, as a regulatory ligand, and competes with the CepIR complex to regulate
105 virulence.
106
107 **Results**
108 *Creation and phenotypic characterization of a* paaK *double mutant*
109 Previously, we demonstrated a link between the attenuation of *B. cenocepacia* K56-2
110 Δ*paaABCDE* and the release of PAA (18). However, the interruption of the pathway at this step
111 could also result in an accumulation of PAA-CoA because PAA is converted to PAA-CoA by a
112 PaaK ligase (Fig. 1). To determine the role of each of these molecules in the attenuation of
113 virulence, we characterized a *paaK* mutant that should only produce PAA and compared it to the
114 *paaABCDE* mutant. Similarly to the reference strain *B. cenocepacia* J2315 (22) in K56-2 there
115 are two similar but not identical phenylacetyl-CoA ligases, PaaK1 and PaaK2 (23). We created

116 marker-less deletion mutants of *paaK1* (BCAL0404) and *paaK2* (BCAM1711). Knockout
117 mutants of the other *paaK* were then made in each background resulting in two independently
118 made double knockouts, which we have named Δ*paaK1*Δ*paaK2* and Δ*paaK2*Δ*paaK1*.
119 To confirm the interruption of the PAA pathway, K56-2 and mutants were grown on LB
120 media and M9 minimal medium with glucose or PAA as a sole carbon source. No growth defect
121 was observed in LB or glucose (Fig. 2A and B). Both *paaK* single knockout mutants were also
122 able to grow on PAA as a sole carbon source to wild type levels, indicating that PAA can be used
123 as a substrate for both ligases (Fig. 2B). While mutants were able to grow normally on glucose as
124 a sole carbon source, the *paaK* double knockout mutants (Δ*paaK1*Δ*paaK2* and Δ*paaK2*Δ*paaK1*)
125 were unable to grow on PAA (Fig. 2B). Growth was complemented with a plasmid containing a
126 rhamnose-inducible *paaK2* (BCAM1711) (Fig. S2) confirming that the interruption of the
127 pathway in these mutants was caused by the deletion of *paaK*. Mutants with full interruption of
128 the pathway (*ΔpaaABCDE*, *ΔpaaK1ΔpaaK2,* and *ΔpaaK2ΔpaaK1*) were unable to grow on PAA
129 as a sole carbon source. Single deletion mutants of the *paaK* ligases (*ΔpaaK1* and *ΔpaaK2*) grew
130 to wild type levels on PAA indicating that the pathway is not interrupted in these strains. The
131 PaaABCDE mutant has been shown to accumulate extracellular PAA due to the interruption of
132 the pathway (18) but the concentration of intracellular PAA and PAA-CoA was unknown.
133 Intracellular and extracellular concentrations of both PAA and PAA-CoA were measured with
134 ion pair reversed phase ultra-high performance liquid chromatography tandem mass
135 spectrometry (IP-RP-UHPLC-MS/MS) using the differential method (24–26). In general, high
136 levels of PAA were found extracellularly rather than intracellularly. The average extracellular
137 concentration of PAA in the wild type, Δ*paaABCDE,* Δ*paaK1*Δ*paaK2,* and Δ*paaK2*Δ*paaK1*
138 supernatants was 37.3, 357.0, 107.3, and 93.9 μM, respectively (Fig. 2C) whereas the average

139 values for intracellular PAA in the same strains were 6.0, 2.0, 1.7 and 8.0 μM (Fig. 2D). When
140 we examined the concentrations of PAA-CoA, we found that the average extracellular levels of
141 PAA-CoA were below or near the limit of detection for all strains, as expected for a CoA
142 molecule that cannot transverse cell membranes. However, PAA-CoA accumulated
143 intracellularly to levels slightly above the limit of detection (Fig. 2E). The intracellular levels of
144 PAA-CoA (Fig. 2F) were higher in Δ*paaABCDE,* (0.94 μM) than in the PaaK mutants (0.54 μM
145 and 0.38 μM). However, the low micromolar amounts detected and the high variability between
146 biological replicates made it challenging to establish clear differences between the PAA-CoA
147 content of the wild type and the PAA degradation mutants.

148 To determine how interruption of each of the two consecutive steps of PAA degradation
149 could affect QS-regulated virulence traits, the killing ability of PAA pathway mutants was
150 compared to wild type in slow killing assays, which quantify the survival of gut-infected
151 nematodes fed on the respective mutants (Fig. 3A). As previously seen, the Δ*paaABCDE*-
152 exposed nematodes had a higher survival rate than those fed on K56-2 ($p < 0.001$). Surprisingly,
153 the nematodes exposed to the Δ*paaK1*Δ*paaK2* mutant showed only 31% (±19%) survival on day
154 2. This was an increase in pathogenicity compared to K56-2, which had 66% (±10%) survival on
155 day 2 ($p < 0.0001$). This virulent phenotype was also observed in nematodes fed with
156 Δ*paaK2*Δ*paaK1* (Fig. S3A) but not in those fed with the single *paaK* deletion mutants (Fig.
157 S3B).

158 To further investigate the opposite virulence phenotypes of the *ΔpaaABCDE* and
159 Δ*paaK1*Δ*paaK2* mutants, we measured the exoprotease activity of both strains, a well-studied
160 virulence trait of *B. cenocepacia* that is regulated by CepIR (10, 27). To ensure that PAA-related
161 metabolites could be produced, we added the precursor phenylalanine to the 2% skim milk agar

162 used for the exoprotease assay, as previously performed (18). In the absence of phenylalanine,
163 the proteolytic activity of the Δ*paaABCDE* mutant was similar to that of K56-2. However, when
164 phenylalanine was added to the medium, the proteolytic activity of Δ*paaABCDE* was abolished
165 (Fig. 3B). On the other hand, the proteolytic activities of Δ*paaK1*Δ*paaK*2 and Δ*paaK2*Δ*paaK1*
166 were higher than that of K56-2, regardless of the addition phenylalanine (Fig. 3B and Fig. S3C).
167 This is in agreement with the results from the slow killing assays where only Δ*paaABCDE* was
168 attenuated for virulence while the Δ*paaK1*Δ*paaK*2 and Δ*paaK2*Δ*paaK1* were more pathogenic
169 than the wild type. Together, we observed no correlation between extracellular levels of PAA
170 and pathogenicity (Fig. S4).
171
172 *PAA-CoA has no effect on CepR and CepI function* in vitro
173 Because PAA-CoA synthesis is interrupted in the *paaK* mutants but not in the
174 *paaABCDE* mutant, we hypothesized that PAA-CoA was responsible for attenuating virulence.
175 As the Δ*paaABCDE* is attenuated for virulence traits that are under the control of the CepIR
176 quorum sensing system (28), we focused our attention on a possible direct effect of PAA-CoA on
177 the CepIR. In addition, Δ*paaABCDE* had decreased *cepI* and *cepR* promoter activity and AHL
178 signaling (18). Specifically, we asked whether PAA-CoA could: 1) inhibit the formation of
179 CepR:AHL complexes; 2) inhibit the enzymatic activity of CepI; and/or 3) indirectly affect an
180 upstream regulator.
181 To address the first question, we built a reporter system (W14/pTL7/pTL5/pTL22
182 referred to from here on as CepR reporter strain, Fig. 4A) similar to those commonly used to
183 identify quorum sensing inhibitors (29). Briefly, *cepR* was expressed under the control of an
184 arabinose-inducible promoter. In the presence of exogenously added AHL, CepR binds to the

185 *cepI* promoter that controls the expression of luminescence genes *luxCDABE*. Addition of an
186 inhibitor would result in decreased expression of luminescence. To test PAA-CoA, PAA was
187 added and converted to PAA-CoA (Fig. 4B) by the action of a PaaK ligase (See supplemental
188 materials for a full description of the reporter system). Using this reporter system we observed
189 that although there was inhibition of luminescence in the presence of PAA-CoA, the level of
190 inhibition was similar to that of the control strains (Fig. 4C). Similarly, PAA itself also had no
191 effect on the system (Fig. 4D). In summary, these results show that PAA-CoA and PAA do not
192 directly affect CepI activity or CepR:C8-HSL formation.

193 To analyze if PAA or PAA-CoA inhibits the enzymatic activity of CepI, we used
194 recombinant CepI in the presence of dichlorophenolindophenol (DCPIP) to
195 spectrophotometrically measure the activity of CepI (30). CepI catalyzes the formation of C8-
196 HSL from octanoyl-Acyl Carrier Protein (C8-ACP) and *S*-adenosyl methionine (SAM). During
197 this reaction DCPIP is reduced resulting in a colour change that can be used to measure activity
198 of CepI. Enzyme activity showed no change in the presence of 200 μM of PAA-CoA or PAA
199 (Table 1), suggesting that neither molecule directly inhibits the activity of CepI.

200 As our data did not show a direct effect of PAA-CoA on the CepIR QS system but *cepI*
201 and *cepR* promoter activity was decreased in the PaaABCDE mutant (18), we hypothesized that
202 PAA-CoA may indirectly affect an upstream regulator of the CepIR QS system. If this was the
203 case, we predicted that the differences in pathogenicity between the Δ*paaABCDE* and the
204 Δ*paaK1*Δ*paaK2* mutant strains would be explained by differential expression of *cepI* and *cepR*.
205 Using stationary phase cultures, we measured the transcript levels of *cepI* and *cepR* and the
206 levels of C8-HSL in the PAA pathway mutants and compared it to wild type. Surprisingly, the
207 Δ*paaABCDE* and the Δ*paaK1*Δ*paaK2* mutants had wild type levels of *cepI* and *cepR*

208 transcription (Fig. 5A and Fig. S5A) despite the striking differences in their virulence
209 phenotypes and contradicting our previous results where reporter systems measured decreased
210 *cepI* and *cepR* promoter activity and decreased AHL signaling (18). This suggested that the
211 attenuation of the Δ*paaABCDE* mutant is independent of the transcription of the CepIR QS
212 system. To confirm the wild type transcription levels of our mutants, we measured the levels of
213 AHL molecules in each strain. Similar to the transcription, the levels of C8-HSL, taken from
214 stationary phase samples did not correlate with the decreased virulence of our PAA pathway
215 mutants (Fig. 5B and Fig. S5B). However, both Δ*cepI* and Δ*cepR* had no measurable C8-HSL
216 which is consistent with their lack of virulence (Fig. 5B).
217
218 *The CepR-independent virulence of PaaK knockout mutants is mediated by the presence/absence*
219 *of PAA-CoA*
220 Transcription of *cepI* and *cepR* is not decreased in PAA pathway mutants and C8-HSL is
221 present in the mutants yet the virulence factors attenuated in the Δ*paaABCDE* mutant
222 (pathogenicity in *C. elegans* and exoprotease activity) are known to be under the control of the
223 CepIR system. To further understand how the PAA pathway may regulate QS-related virulence
224 without affecting *cepIR* transcription, we created marker-less deletions of *cepI* and *cepR* in the
225 PAA pathway deletion mutant backgrounds. We reasoned that if PAA-related regulation of
226 virulence was completely independent of CepI and CepR activity, then deletion of *cepI* and *cepR*
227 in a Δ*paaABCDE* background should show an additive attenuation effect. Similarly, deletion of
228 *cepI* and *cepR* in a Δ*paaK1*Δ*paaK2* mutant background should show the same degree of
229 attenuation as the *cepI* and *cepR* deletions in a wild type background. Once we had created
230 knockout mutants of *cepI* and *cepR* for each PAA pathway mutant in parallel with *cepI* and *cepR*

231 deletions in wild type K56-2, we analyzed their growth and found no defect when grown in LB
232 media over 24 hours (Fig. S6). Next, we used virulence assays to determine if the CepIR QS
233 system was needed for the regulation of their QS. The virulence of the *cepI* and *cepR* knockout
234 mutants in wild type and PAA mutant backgrounds was compared in slow killing assays (Fig. 6A
235 and B, Fig. S7A and B). Both *cep* QS mutants in the Δ*paaABCDE* background were more
236 attenuated for virulence than Δ*paaABCDE* (Fig. S7A). However, they failed to show an additive
237 effect (Fig. S7A). Moreover, while the Δ*paaK1*Δ*paaK2*Δ*cepI* mutant was as attenuated as Δ*cepI*,
238 Δ*paaK1*Δ*paaK2*Δ*cepR* was not, showing that the pathogenic phenotype was independent of
239 CepR (Fig. 6A and B). This was mirrored in the Δ*paaK2*Δ*paaK1*Δ*cepR* mutant (Fig. S7B). This
240 is surprising considering the *cepR* deletion in wild type and the *paaABCDE* mutant has a severe
241 attenuation (Fig. S7A).

242 Corroborating the results of the *C. elegans* assay, Δ*paaK1*Δ*paaK2*Δ*cepR* had wild type
243 levels of proteolytic activity whereas the Δ*paaK1*Δ*paaK2*Δ*cepI* mutant had none (Fig. 6C and
244 Fig. S7C). The only difference between the Δ*paaK1*Δ*paaK2*Δ*cepR* mutant and the *cepR* mutant
245 is the presence of PAA. If PAA was responsible for the elimination of the *cepR* attenuation, the
246 Δ*paaABCDE*Δ*cepR* mutant should be pathogenic but our results show it is not.

247 To further understand the virulence of the Δ*paaK1*Δ*paaK2*Δ*cepR* mutant, we examined
248 the expression levels of *cepI* and *cepR* and the levels of C8-HSL in the mutants. While
249 transcription of *cepR* is abolished in Δ*cepI*, it is restored to wild type levels when the deletion of
250 *cepI* occurs in a Δ*paaK1*Δ*paaK2* or Δ*paaABCDE* background (Fig. 6D and Fig. S7D for
251 Δ*paaK2*Δ*paaK1*). Therefore PAA, which is present in both PAA pathway mutants, restores *cepR*
252 transcription but not pathogenicity, because there is no CepI and no C8-HSL (Fig. 6F). When
253 *cepI* transcript levels were analyzed in Δ*cepR* in wild type and PAA degradation mutant

254 backgrounds, the transcription of *cepI* was downregulated in the CepR mutant, as expected.
255 Similarly, *cepI* transcription was reduced in the attenuated Δ*paaABCDE*Δ*cepR* and the
256 pathogenic Δ*paaK1*Δ*paaK2*Δ*cepR* (Fig. 6E and Fig. S7E for Δ*paaK2*Δ*paaK1*Δ*cepR*). The lack of
257 C8-HSL in both the Δ*paaK1*Δ*paaK2*Δ*cepI* and Δ*paaK1*Δ*paaK2*Δ*cepR* (Fig. 6F) mutants
258 suggests the pathogenicity of the Δ*paaK1*Δ*paaK2*Δ*cepR* mutant is independent of *cepI*. This was
259 mirrored in the Δ*paaK2*Δ*paaK1*Δ*cepR* mutant (Fig. S7F).
260 Deletions of the *cepI* and *cepR* genes in the PAA pathway mutant backgrounds allowed
261 us to determine that the PAA pathway has an effect on CepIR-regulated virulence that is evident
262 when CepI or CepR is absent. In this context, our results suggest that there is an alternative
263 signalling pathway to activate virulence in the Δ*paaK1*Δ*paaK2*Δ*cepR* mutant. The opposite
264 effects of the PaaK and PaaABCDE mutations with regards to pathogenicity and the striking
265 differences that *paaK* and *paaABCDE* gene deletions have in the *cepR* mutant background
266 suggest that PAA-CoA, or a derivative, is the central molecule implicated in this alternative
267 signalling pathway.
268
269 **Discussion**
270 In *B. cenocepacia*, the attenuation of CepIR QS-regulated virulence traits in PAA
271 pathway mutants was thought to be due to the accumulation of PAA (18). In line with this
272 finding, PAA has also been shown to regulate the virulence of other Gram-negative bacteria,
273 *Acinetobacter baumannii* (16) and *Pseudomonas aeruginosa* (31, 32), two Gram-negative
274 bacteria that also use LuxIR-type QS systems to regulate their virulence (33, 34). Previously, we
275 demonstrated that the release of PAA in a *B. cenocepacia* mutant of the PAA pathway resulted in
276 the inhibition of CepIR-regulated QS, a LuxIR-type system (18). However, the Δ*paaABCDE*

277 mutant has the genes necessary to convert PAA to PAA-CoA (Fig. 1). Therefore, PAA or PAA-
278 CoA could be the molecule responsible for the inhibition of CepIR-regulated QS.
279 To determine the molecule responsible, we attempted to create a mutant unable to
280 accumulate PAA-CoA. The PaaK knockout mutant accumulated less PAA-CoA than the
281 Δ*paaABCDE* mutant, and was more virulent than the wild type, suggesting that the attenuated
282 virulence could be due to the accumulation of PAA-CoA, or a derivative. Another difference
283 between these two mutants is that the PaaK knockout mutant released less PAA than the
284 PaaABCDE mutant. Since PAA-CoA is the true inducer of the PAA pathway, the increased
285 accumulation of PAA in the PaaABCDE mutant is likely due to induction of the upstream
286 degradation pathway when PAA-CoA relieves the regulator, PaaR (35). Although our results
287 show that the PaaABCDE mutant produces more PAA than both PaaK1PaaK2 and PaaK2PaaK1
288 mutants, the accumulation of PAA is extracellular. There were no significant differences in the
289 intracellular concentrations of PAA mutants compared with the wild type and the amounts were
290 detected at levels very close to, or lower than, the smallest standard used for the calibration curve
291 (8 μM). Therefore, any effect of PAA on virulence should be attributed to extracellular levels of
292 PAA. However, this does not seem to be the case as exogenous addition of PAA to *B.*
293 *cenocepacia* wild type did not change its pathogenic phenotype (18).
294 We hypothesized CepIR-regulated QS inhibition was achieved by one of three
295 mechanisms: 1) direct inhibition of the enzymatic activity of CepI or its products; 2) inhibition of
296 the formation of CepR:C8-HSL complex; or 3) an indirect effect on an upstream regulator. Using
297 an *E. coli* reporter system that can't metabolize PAA, we examined the ability of PAA-CoA to
298 act as a direct inhibitor of the CepIR QS system. We were able to observe strong but unspecific
299 inhibition of luminescence by PAA and PAA-CoA, highlighting the importance of control strains

300 when reporter systems are used to identify QS inhibitors: QS-regulated phenotypes often depend
301 on other factors; and reporter strains using bioluminescence can be affected by the overall
302 metabolic activity of the cell (29). In our system, the control strains had either the arabinose-
303 inducible P_{BAD} promoter or the *dhfr* constitutive promoter controlling the expression of
304 *luxCDABE* luminescence genes. First, in the presence of higher concentrations of PAA (above 1
305 mM) the expression of luminescence by the constitutive promoter was inhibited suggesting a
306 general effect on luminescence. Second, the concentration of rhamnose used to express *paaK,*
307 0.01% w/v, inhibited the arabinose-inducible promoter. With these control strains, we were able
308 to minimize the general effects on the reporter system and determine that neither PAA or PAA-
309 CoA have a direct effect on the formation of CepR:C8-HSL complexes or on CepI activity.
310 Interestingly, we found that the attenuation of virulence in Δ*paaABCDE* did not
311 correspond to decreased *cepI* and *cepR* transcription or C8-HSL production. The lack of
312 downregulation of either *cepI* or *cepR* in the Δ*paaABCDE* mutant was quite surprising because
313 this contradicted the results from our plasmid-based reporter systems that showed decreased *cepI*
314 and *cepR* promoter activity and decreased AHL signalling (18). To investigate this discrepancy,
315 we introduced the plasmids with P_{cepI}::*luxCDABE* or P_{cepR}::*luxCDABE* to the Δ*paaK1*Δ*paaK2*
316 and Δ*paaK2*Δ*paaK1* mutants and found decreased *cepI* and *cepR* promoter activity almost
317 identical to that of the Δ*paaABCDE* mutant with the same plasmid-based reporter system (data
318 not shown). This suggests that the PAA present in both these mutants might have had a general
319 effect on the reporter system itself. It is possible that PAA may affect the copy number of the
320 plasmid or affect the metabolism of the cells in such a way that affects plasmid-based reporter
321 strains as previously shown in *E. coli* (36).

322 We initially focused our attention on *B. cenocepacia* CepIR because this QS system
323 solely controls pathogenicity in *C. elegans* where the virulence attenuation of PAA degradation
324 mutants was first characterized (22). However, current evidence suggests that a two-component
325 system, RqpSR, is at the top of the hierarchy controlling both AHL- and BDSF-dependent QS
326 systems (37, 38) . The BDSF-dependent system uses cis-2-dodecenoic acid signalling molecule
327 (*Burkholderia* diffusible signal factor or BDSF) that regulates overlapping genes with the AHL
328 QS system (39). We considered that the virulence of the Δ*paaABCDE* may be attenuated through
329 an indirect effect. However, RqpSR and BDSF both regulate the expression of *cepI*, which is not
330 differentially regulated in the Δ*paaABCDE* mutant, nor was there decreased production of AHLs
331 (37, 40). To determine if the attenuated virulence of Δ*paaABCDE* could be independent of CepI
332 and CepR activity we created *cepI* and *cepR* mutants in the PAA pathway mutant backgrounds.
333 If PAA-related regulation of virulence was independent of CepI and CepR activity, then we
334 would see an additive effect on attenuation. Whereas, in a *paaK* knockout mutant background we
335 expected to see a virulence phenotype similar to that of the same deletion in a wild type strain. In
336 the Δ*paaABCDE* QS mutants we saw no evidence of an additive effect as the QS mutations were
337 dominant, leading to the same pathogenicity as a wild type Δ*cepI* or Δ*cepR* mutant. Because the
338 *cepI/R* mutations in Δ*paaABCDE* did not have an additive effect, this suggests the mechanism of
339 attenuation involves the CepIR QS system without affecting the expression of the *cepI/R* genes.
340 Recently, an analogue of BDSF was shown to inhibit the production of AHL signals in *B.*
341 *cenocepacia* H111 (38). In the future, it would be interesting to test the ability of the compound
342 to inhibit QS-regulated virulence in a genetic background where PAA-CoA synthesis is
343 interrupted.

344 In the *paaK* knockout background the QS mutations had opposing effects. While a *cepI*
345 deletion resulted in the expected attenuated virulence, a *cepR* deletion had wild type levels of
346 virulence. Surprisingly, the PAA pathway mutants with a *cepI* deletion had increased
347 transcription of *cepR.* Therefore, it seems that extracellular PAA, observed in both PAA pathway
348 mutants, can restore the transcription of *cepR* to wild type levels. While increased transcription
349 of *cepR* by PAA may suggest that this is the reason why the *paaK* mutants are more pathogenic
350 than the wild type, it does not explain why PAA does not produce the same effect in the
351 *paaABCDE* mutant nor does explain why the *cepR* mutation in a *paaK* background reverts to
352 wild type levels of virulence. A possible reason for these striking opposite phenotypes, is that in
353 the *paaK* mutants a regulatory component is activated in the absence of CepR. We speculate that
354 this activation is sensitive to the levels of PAA-CoA. However, a limitation of our work is that
355 we were unable to detect statistically significant differences between the levels of PAA-CoA in
356 wild type and PaaK mutants as the amounts of PAA-CoA were very close to the limit of
357 detection of our method.
358 Finally, the results presented here highlight how changes in a catabolic pathway can
359 modulate virulence in bacteria. Variations in the concentration of PAA-CoA led to CepR-
360 dependent attenuated virulence, despite the presence of CepR. Conversely, the same virulence
361 factors could increase, despite the absence of CepR. We propose that increased virulence due to
362 PAA metabolites may be relevant in environmental conditions where quorum sensing signals do
363 not accumulate but a virulent response is necessary.
364

365 **Materials and Methods**

366 *Strains, media preparation and growth conditions*

367 Bacterial strains, listed in Table 2, were grown at 37°C with agitation at 230 rpm in
368 Lysogeny Broth (LB) Lennox medium (without glucose) (41), unless specified. All cultures were
369 started from isolated colonies grown 48 hours on LB agar at 37°C, unless specified. Plasmids
370 used are listed in Table 3. For *E. coli* strains the following antibiotics and concentrations were
371 used: Ampicillin (100 µg/ml; 200 µg/ml for W14 strain); Chloramphenicol (30 µg/ml),
372 Kanamycin (30 µg/ml; 40 µg/ml for MM290 strain), Trimethoprim (50 µg/ml; 100 µg/ml for
373 W14 strain), Tetracycline (20 µg/ml). For *B. cenocepacia* strains the following antibiotics and
374 concentrations were used: Trimethoprim (100 µg/ml), Tetracycline (100 µg/ml), Gentamycin (50
375 µg/ml). Stock solutions of C8-HSL (Sigma Aldrich), were suspended in dimethyl sulfoxide
376 (DMSO) and stored at -20°C. For assays with exogenous addition of C8-HSL cultures were
377 grown in LB supplemented with 50 mM 3-(*N*-morpholino)propanesulfonic acid (MOPS) to
378 prevent pH-dependent lactonolysis (42). Stock solutions of L-arabinose (Alfa Aesar, Fisher
379 Scientific) and L-rhamnose (Sigma Aldrich) were prepared at a concentration of 20% (w/v) in
380 deionized water and filter sterilized. Stock solutions of phenylalanine and PAA (Sigma Aldrich)
381 were prepared at 100 mM in deionized water, filter sterilized and stored at room temperature.
382 Stock solutions of PAA-CoA (Sigma Aldrich) were prepared at 3.5 mM in DMSO and stored at -
383 80°C.
384
385 *Molecular biology techniques*
386 Genetic manipulation of *B. cenocepacia* K56-2 was performed via tri-parental matings
387 with *E. coli* MM290/pRK2013 as a helper strain. Plasmids generated were maintained in *E. coli*
388 SY327λpir or DH5α Z-competent cells depending on their origin of replication. PCRs were
389 performed with an Eppendorf Mastercycler ep gradient S thermocycler with either HotStar

390 HiFidelity *Taq* polymerase (Qiagen) or *Taq* DNA polymerase (Qiagen). Conditions were
391 optimized for each primer set; primers used are listed in Table 4. Restriction enzymes and T4
392 DNA ligase (New England Biolabs) were used as recommended by the manufacturer. PCR
393 products and digested DNA were purified by QIAquick Gel or PCR purification kits (Qiagen)
394 and plasmids were isolated using QIAprep Miniprep kit (Qiagen).
395 *Construction of unmarked deletion mutants in B. cenocepacia*
396 Unmarked deletion mutants were created using the system developed by Flannagan *et al*.
397 (48). Flanking regions of the target gene were synthesized as a custom gene fragment with *Xba*I
398 and *Sma*I restriction sites (Integrated DNA Technologies, Inc.), see Table S1 for sequences. The
399 fragment with regions flanking BCAL0404 (*paaK1*) and pGPI-*Sce*I were digested and ligated
400 together to create pTL17 and pTL18 was created by insertion of the fragment with regions
401 flanking BCAM1711 (*paaK2*). Each plasmid was introduced into wild type K56-2 by tri-parental
402 mating and were integrated into the genome by homologous recombination. Colonies were
403 picked onto LB medium supplemented with trimethoprim and onto *Burkholderia cepacia*
404 selective agar (BCSA) (54). Conjugates with a dull phenotype on BCSA were selected. The
405 integration of the suicide plasmids was confirmed with primers 900/901 for pTL17 and primers
406 902/903 for pTL18. Then, pDAI-*Sce*I, expressing I-*Sce*I endonuclease, was introduced into K56-
407 2::pTL17 and K56-2::pTL18 by tri-parental mating. The double-stranded break caused by the I-
408 *Sce*I endonuclease triggered a recombination event that resulted in a reversion of the conjugate to
409 a wild type allele or a deletion of the fragment between the two flanking regions. Potential
410 conjugates were tetracycline resistant and trimethoprim sensitive. The deletion event was
411 confirmed by PCR using primer set 980/981 for *paaK1* and 982/983 for *paaK2*. Positive clones
412 were cured of the pDAI-*Sce*I plasmid by sequential sub-culturing in LB medium. Loss of the

413 plasmid was confirmed by the loss of tetracycline resistance using the replica plate method and
414 PCR with primer set 920/921 for the absence of pDAI-*Sce*I.
415 Once cured, the mutants were tested for growth defects by washing overnight cultures
416 twice in PBS, diluting to an OD_{600} of 0.04 in 200 µl of LB in a clear 96-well plate in triplicate.
417 Plates were incubated at 37°C in a Biotek Synergy II plate reader with continuous shaking for 24
418 hours with OD_{600} measured every hour. Deletions of *cepI* and *cepR* were performed in the wild
419 type and PAA pathway mutant backgrounds using the pDelCepI and pDelCepR plasmids created
420 by Aubert *et al.* (53). Integration of the plasmids was confirmed using primer set 1082/154 for
421 *cepI* deletions and 1080/154 for *cepR*. pDAI-*Sce*I was introduced and potential conjugates were
422 selected on appropriate antibiotics and the deletion event was confirmed by PCR with primer sets
423 1112/1113 and 1080/1081 for *cepI* and *cepR*, respectively. Positive clones were cured of the
424 pDAI-*Sce*I and screened for the loss of the plasmid as described above.
425
426 *Plasmid construction*
427 To create pKF2, *paaK2* (BCAM1711) was amplified from genomic *B. cenocepacia* K56-
428 2 DNA using primers 1055/1056 and restricted with *Xba*I and *Nde*I before ligation into similarly
429 digested pSCrhaB2 (52). The plasmid construct was verified using primers 1055/848. To create
430 the *E. coli* reporter system, *cepR* (BCAM1868) was amplified using primers 703/704 and the
431 amplicon and pBAD30 were restricted with *Eco*RI and *Xba*I and then ligated to form pTL5. To
432 construct a plasmid expressing the *luxCDABE* operon, the *cepI* promoter region including the
433 first 15 codons of *cepI* was amplified and an in-frame stop codon was added using primers 712
434 and 713. Plasmid pBBRlux and the amplicon were digested with *Spe*I and *Bam*HI, and ligation
435 then resulted in pTL7. Plasmids pTL12 and pTL13 were created in the same way with primers

436 768/769 for the P_{BAD} promoter and regulatory *araC* and primers 770/771 for the *dhfr* promoter
437 region of pTnMod-STp. To create a plasmid that expressed PaaK and was compatible with the
438 reporter strain we had to use the pSC101 ori. pTL9 was created by digesting pTnMod-STp with
439 *Bgl*II to remove the Tn*5* transposase, then the rhamnose inducible promoter and its regulatory
440 genes were added to create pTL21 using primers 724 and 947. Using primers 725 and 726 the
441 *paaK* ligase from *E. coli* W was amplified from pAAD (45) and restriction cloned into pTL21 to
442 create pTL22.
443
444 *Growth of* B. cenocepacia *strains on various carbon sources*
445 One ml of culture from a five-ml overnight culture in LB with appropriate antibiotic was
446 washed in PBS twice and the OD_{600} was adjusted to 0.08 in 1 ml of M9 with 25 mM of Glucose
447 or M9 with 5 mM PAA. 100 µl was aliquoted to each well of a clear 96-well plate with 100 µl of
448 appropriate media for a starting OD_{600} of 0.04 in triplicate. Plates were incubated at 37°C with
449 aeration at 230 rpm and the OD_{600} was read after 48 hours of incubation. OD_{600} values were
450 converted to 1-cm-path-length by prior calibration with a GeneQuant™ III 4283, version
451 4283V1.6.
452
453 *Quantification of intracellular and extracellular levels of PAA and PAA-CoA by ion pair*
454 *reversed phase ultra-high performance liquid chromatography tandem mass spectrometry (IP-*
455 *RP-UHPLC-MS/MS)*
456 *B. cenocepacia* cultures were diluted 1:100 into 10 ml of LB broth in a 50 ml Erlenmeyer
457 flask and incubated at 37°C with agitation at 230 rpm for 6 hours until late exponential phase.
458 Using the differential method (24, 25), 1 ml of culture was immediately transferred into weighed

459 tubes containing 5 ml of 60% (v/v) methanol in water held at -40°C in an acetonitrile/dry-ice
460 bath, vortexed and returned to -40°C. Two ml of culture was drawn into a syringe, equipped with
461 a 0.45 µm filter, and 1 ml of filtrate was immediately transferred into 5 ml of 60% (v/v)
462 methanol in water held at -40°C in an acetonitrile/dry-ice bath, vortexed and returned to -40°C.
463 Tubes were weighed and 500 µl was transferred to a fresh tube and held at -40°C. 5 ml of 75%
464 (v/v) ethanol was boiled at 95°C for 4 minutes and then poured into the tube with 500 µl of
465 sample, mixed and placed at 95°C for 3 minutes. Extracted samples were then put back at -40°C
466 and evaporated in a speedvac (Savant SC110 with refrigerated condensation trap RT100) until
467 dry. Care was taken to ensure that the samples were not overdried. All measurements were
468 carried out using IP-RP-UHPLC-MS/MS as described previously (26) with slight modifications.
469 Briefly, no splitter or make up flow was used and the chromatographic separation was performed
470 on a narrower column (1x100 mm) with a lower eluant flow (0.075 ml/min).
471 For the *E. coli* W14 CepR reporter assay strains, cultures were diluted 1:100 in 5 ml of
472 LB supplemented with 50 mM MOPS and appropriate antibiotics and grown at 30°C, 230 rpm to
473 OD_{600} ~ 0.3. Cultures were provided 0.5 mM PAA and 0.01% rhamnose to induce the expression
474 of *paaK* to convert PAA to PAA-CoA. Cultures were incubated again until an OD_{600} of 0.6 and
475 diluted back to OD_{600} 0.3 before incubation for 1h30 minutes to simulate the conditions of the
476 reporter assay. Samples were immediately prepared using the differential method described
477 above.
478
479 *Slow killing assays in* Caenorhabditis elegans
480 Worms were propagated and maintained on nematode growth medium (NGM) agar (2.5
481 g peptone/l) seeded with a lawn of *E. coli* OP50 at 16°C. Slow killing assays were performed as

482 described previously (18). Briefly, 60-mm Petri plates filled with 10 ml of a modified NGM agar
483 (3.5 g peptone/l) were seeded with 50 µl of a stationary-phase culture adjusted to an OD_{600} of
484 1.7. Plates were incubated overnight at 37°C to allow formation of a bacterial lawn. 20 to 40
485 hypochlorite-synchronized *C. elegans* DH26 nematodes at L4 larval stage were inoculated onto
486 each plate and subsequently incubated at 25°C for the duration of the assay. Worms were scored
487 as live or dead for a period of 7 days.
488
489 *Exoprotease assays*
490 Cells from an overnight culture were washed with PBS twice and adjusted to an OD_{600} of
491 1.0. Three microliters of culture were spotted on 2% skim milk agar plates or 2% skim milk agar
492 supplemented with 2 mM phenylalanine. Plates were incubated at 37°C for 48 hours. Plates were
493 prepared in duplicate and three biological replicates were performed. Proteolytic activity was
494 measured as a zone of clearing surrounding the colony. Images were taken at 48 hours and the
495 area of the zone of clearance was analyzed using ImageJ software (55). A scale was applied to
496 the images and a threshold analysis was used to determine the zone of clearance. The area of this
497 zone was then calculated (minus the area of the colony).
498
499 *CepI enzymatic assay*
500 Heterologous expression and purification of *cepI* was performed according to the
501 conditions described previously (30). CepI enzyme activity was determined
502 spectrophotometrically by measuring *holo*-ACP formation with dichlorophenylindophenol
503 (DCPIP; = 19100 M-1 cm-1) using the assay described previously (30, 56). Reaction mixtures
504 contained 50 mM 4-(2-hydroxyethyl)-1-piperazineethanesulfonic acid (HEPES) pH 7.5, 0.005%

505 Nonidet P-40, 0.13 mM DCPIP, 70 μM C8-ACP, 4 μM CepI. After 10 minutes of pre-incubation
506 the reaction was initiated by addition of 40 μM S-adenosyl methionine. The compounds were
507 assayed in triplicate at a concentration of 200 μM.
508
509 *Luminescence assays with CepR reporter strain*
510 The reporter assay was performed based on the assay by McInnis and Blackwell (57)
511 with slight modifications. Briefly, overnight cultures were prepared from glycerol stocks in LB
512 with appropriate antibiotics and incubated overnight at 30°C with agitation at 230 rpm. The
513 culture was diluted 1:100 into 5 ml fresh LB medium supplemented with 50 mM MOPS and
514 appropriate antibiotics. This subculture was incubated at 30°C with shaking at 230 rpm until it
515 reached an optical density of 0.6. One hundred microliters of culture were plated into wells with
516 100 μl of appropriate media with C8-HSL, PAA and arabinose as needed, resulting in a starting
517 OD_{600} of 0.3. For the reporter strain with pTL22 (rha-inducible *paaK*) the culture was grown and
518 subcultured as described above. This subculture was incubated at 30°C with shaking at 230 rpm
519 until it reached an optical density of ~0.3. At this time 0.5 mM PAA and 0.01% rhamnose were
520 added to induce *paaK* expression resulting in the conversion of PAA to PAA-CoA. The cultures
521 were incubated at 30°C, 230 rpm until an OD_{600} of 0.6. One hundred microliters of culture were
522 plated into wells with 100 μl of appropriate media with C8-HSL, PAA, and arabinose and
523 rhamnose as needed, resulting in a starting OD_{600} of 0.3. Arabinose and rhamnose were used at
524 final concentrations of 0.2% (v/v) and 0.01% (v/v), respectively. C8-HSL was used at a final
525 concentration of 20 nM, which was the EC_{50} of C8-HSL for the conditions of this assay as
526 determined using a dose response curve (Supplemental Fig. S1). PAA was tested at several
527 concentrations (100 μM, 500 μM, 1 mM and 5 mM) and PAA was added at 500 μM in the

528 presence of 0.01% rhamnose to produce PAA-CoA. White 96-well microplates with clear
529 bottoms were used and the lids were treated with a TritonX-100/Ethanol solution. Plates were
530 incubated at 30°C with agitation in a Biotek Synergy 2 plate reader. OD_{600} and relative
531 luminescence were measured at 30 min intervals for 4 h. Inhibition was measured at the time
532 point with peak signal intensity (2 h for PAA and 3 h for PAA-CoA).
533
534 *Reverse Transcription quantitative PCR (RT-qPCR)*
535 Since quorum sensing is associated with cell density, the expression levels of quorum
536 sensing genes are often measured during stationary phase (58–60). To study the expression of
537 *cepI* and *cepR*, *B. cenocepacia* cells were harvested from stationary cultures (OD_{600} ~7). RNA
538 was purified and DNase treated using the Ribopure bacteria kit (Ambion) with the DNase
539 treatment extended to 2 h. RNA quality was confirmed by running on a 2% agarose gel. cDNA
540 was synthesized using iScript Reverse Transcriptase kit (Bio-Rad) and quantified using iQ
541 SYBR Green mastermix (Bio-Rad) performed on a CFX96 Touch Real-Time PCR Detection
542 System (Bio-Rad). Primer efficiency was calculated for each primer set and efficiencies between
543 95% and 105% were deemed acceptable. Data were analyzed using the comparative C_T method
544 (61, 62). Genes were normalized to the RNA polymerase sigma factor *rpoD* (BCAM0918,
545 formerly known as *sigE*) as a reference gene (primers 750 and 751) (7, 63, 64).
546
547 *LC-MS/MS quantification of AHLs*
548 For AHL extraction, five milliliters of *B. cenocepacia* strains were harvested at the same
549 time as the samples used for RT-qPCR (see above). Samples were extracted and analyzed as

550 described previously (65) and 5,6,7,8-Tetradeutero-4-hydroxy-2-heptylquinoline (HHQ-d4) was
551 used as an internal standard at a concentration of 0.2 ppm.
552
553 **Acknowledgements**
554 This study was supported by a discovery grant from the Natural Sciences and Engineering
555 Research Council of Canada (NSERC) awarded to S.T. Cardona. The authors would like to
556 acknowledge the preliminary work of Samuel J. Wolfram, Vincent Henega and Stacey Line. The
557 authors thank Dr. Miguel Valvano for generously sharing plasmids pDelCepR and pDelCepI.
558 pBBRlux was a gift from Dr. Aleksandra Sikora. TJL and STC were responsible for the
559 experimental design and writing the manuscript. TJL and KLF performed the experimental work.
560 CR detected PAA and PAA-CoA using IP-RP-UHPLC-MS/MS. SB and LRC performed the
561 CepI enzyme activity assay. MCG and ED performed the LC-MS/MS and data analysis for AHL
562 quantification. JLS provided knowledge and equipment for the initial detection of PAA by HPLC
563 and edited the manuscript.
564

565 **References**

566 1. Bassler BL. 1999. How bacteria talk to each other: regulation of gene expression by
567 quorum sensing. Curr Opin Microbiol 2:582–587.

568 2. Fuqua WC, Winans SC, Greenberg EP. 1994. Quorum sensing in bacteria: the LuxR-LuxI
569 family of cell density-responsive transcriptional regulators. J Bacteriol 176:269–275.

570 3. Hanzelka BL, Greenberg EP. 1995. Evidence that the N-terminal region of the *Vibrio*
571 *fischeri* LuxR protein constitutes an autoinducer-binding domain. J Bacteriol 177:815–817.

572 4. Winzer K, Williams P. 2001. Quorum sensing and the regulation of virulence gene
573 expression in pathogenic bacteria. Int J Med Microbiol IJMM 291:131–143.

574 5. Mahenthiralingam E, Urban TA, Goldberg JB. 2005. The multifarious, multireplicon
575 *Burkholderia cepacia* complex. Nat Rev Microbiol 3:144–156.

576 6. Darling P, Chan M, Cox AD, Sokol PA. 1998. Siderophore production by cystic fibrosis
577 isolates of *Burkholderia cepacia*. Infect Immun 66:874–877.

578 7. O'Grady EP, Viteri DF, Malott RJ, Sokol PA. 2009. Reciprocal regulation by the CepIR
579 and CciIR quorum sensing systems in *Burkholderia cenocepacia*. BMC Genomics 10:441.

580 8. Malott RJ, Baldwin A, Mahenthiralingam E, Sokol PA. 2005. Characterization of the cciIR
581 quorum-sensing system in *Burkholderia cenocepacia*. Infect Immun 73:4982–4992.

582 9. Lewenza S, Sokol PA. 2001. Regulation of ornibactin biosynthesis and *N*-acyl-L-
583 homoserine lactone production by CepR in *Burkholderia cepacia*. J Bacteriol 183:2212–
584 2218.

585 10. Lewenza S, Conway B, Greenberg EP, Sokol PA. 1999. Quorum sensing in *Burkholderia*
586 *cepacia*: identification of the LuxRI homologs CepRI. J Bacteriol 181:748–756.

587 11. Malott RJ, O'Grady EP, Toller J, Inhülsen S, Eberl L, Sokol PA. 2009. A *Burkholderia*
588 *cenocepacia* orphan LuxR homolog is involved in quorum-sensing regulation. J Bacteriol
589 191:2447–2460.

590 12. Brown SA, Palmer KL, Whiteley M. 2008. Revisiting the host as a growth medium. Nat
591 Rev Microbiol 6:657–666.

592 13. Eisenreich W, Dandekar T, Heesemann J, Goebel W. 2010. Carbon metabolism of
593 intracellular bacterial pathogens and possible links to virulence. Nat Rev Microbiol 8:401–
594 412.

595 14. Fuchs TM, Eisenreich W, Heesemann J, Goebel W. 2012. Metabolic adaptation of human
596 pathogenic and related nonpathogenic bacteria to extra- and intracellular habitats. FEMS
597 Microbiol Rev 36:435–462.

598 15. de Lorenzo V. 2014. From the selfish gene to selfish metabolism: revisiting the central
599 dogma. BioEssays News Rev Mol Cell Dev Biol 36:226–235.

600 16. Bhuiyan MS, Ellett F, Murray GL, Kostoulias X, Cerqueira GM, Schulze KE, Mahamad
601 Maifiah MH, Li J, Creek DJ, Lieschke GJ, Peleg AY. 2016. *Acinetobacter baumannii*
602 phenylacetic acid metabolism influences infection outcome through a direct effect on
603 neutrophil chemotaxis. Proc Natl Acad Sci U S A 113:9599–9604.

604 17. Bartz FE, Glassbrook NJ, Danehower DA, Cubeta MA. 2012. Elucidating the role of the
605 phenylacetic acid metabolic complex in the pathogenic activity of *Rhizoctonia solani*
606 anastomosis group 3. Mycologia 104:793–803.

607 18. Pribytkova T, Lightly TJ, Kumar B, Bernier SP, Sorensen JL, Surette MG, Cardona ST.
608 2014. The attenuated virulence of a *Burkholderia cenocepacia paaABCDE* mutant is due to
609 inhibition of quorum sensing by release of phenylacetic acid. Mol Microbiol 94:522–536.

610 19. Teufel R, Mascaraque V, Ismail W, Voss M, Perera J, Eisenreich W, Haehnel W, Fuchs G.
611 2010. Bacterial phenylalanine and phenylacetate catabolic pathway revealed. Proc Natl
612 Acad Sci U S A 107:14390–14395.

613 20. Teufel R, Friedrich T, Fuchs G. 2012. An oxygenase that forms and deoxygenates toxic
614 epoxide. Nature 483:359–362.

615 21. Lightly TJ, Phung RR, Sorensen JL, Cardona ST. 2017. Synthetic cystic fibrosis sputum
616 medium diminishes *Burkholderia cenocepacia* antifungal activity against *Aspergillus*
617 *fumigatus* independently of phenylacetic acid production. Can J Microbiol 1–12.

618 22. Law RJ, Hamlin JNR, Sivro A, McCorrister SJ, Cardama GA, Cardona ST. 2008. A
619 functional phenylacetic acid catabolic pathway is required for full pathogenicity of
620 *Burkholderia cenocepacia* in the *Caenorhabditis elegans* host model. J Bacteriol 190:7209–
621 7218.

622 23. Imolorhe IA, Silvia TC. 2011. 3-Hydroxyphenylacetic Acid Induces The *Burkholderia*
623 *cenocepacia* Phenylacetic Acid Degradation Pathway. Towards Understanding The
624 Contribution Of Aromatic Catabolism To Pathogenesis. Front Cell Infect Microbiol 1.

625 24. Taymaz-Nikerel H, de Mey M, Ras C, ten Pierick A, Seifar RM, van Dam JC, Heijnen JJ,
626 van Gulik WM. 2009. Development and application of a differential method for reliable
627 metabolome analysis in *Escherichia coli*. Anal Biochem 386:9–19.

628 25. Van Gulik WM, Canelas AB, Taymaz-Nikerel H, Douma RD, de Jonge LP, Heijnen JJ.
629 2012. Fast sampling of the cellular metabolome. Methods Mol Biol Clifton NJ 881:279–
630 306.

631 26. Seifar RM, Ras C, Deshmukh AT, Bekers KM, Suarez-Mendez CA, da Cruz ALB, van
632 Gulik WM, Heijnen JJ. 2013. Quantitative analysis of intracellular coenzymes in
633 *Saccharomyces cerevisiae* using ion pair reversed phase ultra high performance liquid
634 chromatography tandem mass spectrometry. J Chromatogr A 1311:115–120.

635 27. Sokol PA, Sajjan U, Visser MB, Gingues S, Forstner J, Kooi C. 2003. The CepIR Quorum-
636 Sensing System Contributes to the Virulence of *Burkholderia cenocepacia* Respiratory
637 Infections. Microbiology 149:3649–3658.

638 28. Uehlinger S, Schwager S, Bernier SP, Riedel K, Nguyen DT, Sokol PA, Eberl L. 2009.
639 Identification of specific and universal virulence factors in *Burkholderia cenocepacia*
640 strains using multiple infection hosts. Infect Immun 9:4102–4110.

641 29. Defoirdt T, Brackman G, Coenye T. 2013. Quorum sensing inhibitors: how strong is the
642 evidence? Trends Microbiol 21:619–624.

643 30. Scoffone VC, Chiarelli LR, Makarov V, Brackman G, Israyilova A, Azzalin A, Forneris F,
644 Riabova O, Savina S, Coenye T, Riccardi G, Buroni S. 2016. Discovery of new

645 diketopiperazines inhibiting *Burkholderia cenocepacia* quorum sensing in vitro and in vivo.
646 Sci Rep 6:32487.

647 31. Musthafa KS, Sivamaruthi BS, Pandian SK, Ravi AV. 2012. Quorum sensing inhibition in
648 *Pseudomonas aeruginosa* PAO1 by antagonistic compound phenylacetic acid. Curr
649 Microbiol 65:475–480.

650 32. Wang J, Dong Y, Zhou T, Liu X, Deng Y, Wang C, Lee J, Zhang LH. 2013. *Pseudomonas*
651 *aeruginosa* cytotoxicity is attenuated at high cell density and associated with the
652 accumulation of phenylacetic acid. PloS One 8:e60187.

653 33. Niu C, Clemmer KM, Bonomo RA, Rather PN. 2008. Isolation and Characterization of an
654 Autoinducer Synthase from *Acinetobacter baumannii*. J Bacteriol 190:3386–3392.

655 34. Latifi A, Winson MK, Foglino M, Bycroft BW, Stewart GS, Lazdunski A, Williams P.
656 1995. Multiple homologues of LuxR and LuxI control expression of virulence determinants
657 and secondary metabolites through quorum sensing in *Pseudomonas aeruginosa* PAO1.
658 Mol Microbiol 17:333–343.

659 35. Yudistira H, McClarty L, Bloodworth RA, Hammond SA, Butcher H, Mark BL, Cardona
660 ST. 2011. Phenylalanine induces *Burkholderia cenocepacia* phenylacetic acid catabolism
661 through degradation to phenylacetyl-CoA in synthetic cystic fibrosis sputum medium.
662 Microb Pathog 51:183–196.

663 36. Sobotková L, Grafková J, Kyslík P. 2002. Effect of phenylacetic acid on the growth and
664 production of penicillin G acylase of recombinant and host strains derived from *Escherichia*
665 *coli* W. Enzyme Microb Technol 31:992–999.

666 37. Cui C, Yang C, Song S, Fu S, Sun X, Yang L, He F, Zhang L-H, Zhang Y, Deng Y. 2018.
667 A novel two-component system modulates quorum sensing and pathogenicity in
668 *Burkholderia cenocepacia*. Mol Microbiol 108:32–44.

669 38. Cui C, Song S, Yang C, Sun X, Huang Y, Li K, Zhao S, Zhang Y, Deng Y. 2019.
670 Disruption of Quorum Sensing and Virulence in *Burkholderia cenocepacia* by a Structural
671 Analogue of the cis-2-Dodecenoic Acid Signal. Appl Environ Microbiol 85.

672 39. Schmid N, Pessi G, Deng Y, Aguilar C, Carlier AL, Grunau A, Omasits U, Zhang L-H,
673 Ahrens CH, Eberl L. 2012. The AHL- and BDSF-Dependent Quorum Sensing Systems
674 Control Specific and Overlapping Sets of Genes in *Burkholderia cenocepacia* H111. PLOS
675 ONE 7:e49966.

676 40. Deng Y, Lim A, Wang J, Zhou T, Chen S, Lee J, Dong YH, Zhang LH. 2013. Cis-2-
677 dodecenoic acid quorum sensing system modulates N-acyl homoserine lactone production
678 through RpfR and cyclic di-GMP turnover in *Burkholderia cenocepacia*. BMC Microbiol
679 13:148-2180-13–148.

680 41. Lennox ES. 1955. Transduction of linked genetic characters of the host by bacteriophage
681 P1. Virology 1:190–206.

682 42. Yates EA, Philipp B, Buckley C, Atkinson S, Chhabra SR, Sockett RE, Goldner M,
683 Dessaux Y, Cámara M, Smith H, Williams P. 2002. N-Acylhomoserine Lactones Undergo
684 Lactonolysis in a pH-, Temperature-, and Acyl Chain Length-Dependent Manner during
685 Growth of *Yersinia pseudotuberculosis* and *Pseudomonas aeruginosa*. Infect Immun
686 70:5635–5646.

687 43. Mahenthiralingam E, Coenye T, Chung JW, Speert DP, Govan JR, Taylor P, Vandamme P.
688 2000. Diagnostically and experimentally useful panel of strains from the *Burkholderia*
689 *cepacia* complex. J Clin Microbiol 38:910–913.

690 44. Miller VL, Mekalanos JJ. 1988. A novel suicide vector and its use in construction of
691 insertion mutations: osmoregulation of outer membrane proteins and virulence determinants
692 in *Vibrio cholerae* requires *toxR*. J Bacteriol 170:2575–2583.

693 45. Ferrandez A, Prieto MA, Garcia JL, Diaz E. 1997. Molecular characterization of PadA, a
694 phenylacetaldehyde dehydrogenase from *Escherichia coli*. FEBS Lett 406:23–27.

695 46. Ferrandez A, Minambres B, Garcia B, Olivera ER, Luengo JM, Garcia JL, Diaz E. 1998.
696 Catabolism of phenylacetic acid in *Escherichia coli*. Characterization of a new aerobic
697 hybrid pathway. J Biol Chem 273:25974–25986.

698 47. Figurski DH, Helinski DR. 1979. Replication of an origin-containing derivative of plasmid
699 RK2 dependent on a plasmid function provided in trans. Proc Natl Acad Sci U S A
700 76:1648–1652.

701 48. Flannagan RS, Linn T, Valvano MA. 2008. A system for the construction of targeted
702 unmarked gene deletions in the genus *Burkholderia*. Environ Microbiol 10:1652–1660.

703 49. Guzman LM, Belin D, Carson MJ, Beckwith J. 1995. Tight regulation, modulation, and
704 high-level expression by vectors containing the arabinose PBAD promoter. J Bacteriol
705 177:4121–30.

706 50. Zielke RA, Simmons RS, Park BR, Nonogaki M, Emerson S, Sikora AE. 2014. The type II
707 secretion pathway in *Vibrio cholerae* is characterized by growth phase-dependent
708 expression of exoprotein genes and is positively regulated by sigmaE. Infect Immun
709 82:2788–2801.

710 51. Dennis JJ, Zylstra GJ. 1998. Plasposons: modular self-cloning minitransposon derivatives
711 for rapid genetic analysis of gram-negative bacterial genomes. Appl Environ Microbiol
712 64:2710–2715.

713 52. Cardona ST, Valvano MA. 2005. An expression vector containing a rhamnose-inducible
714 promoter provides tightly regulated gene expression in *Burkholderia cenocepacia*. Plasmid
715 54:219–228.

716 53. Aubert DF, O'Grady EP, Hamad MA, Sokol PA, Valvano MA. 2013. The *Burkholderia*
717 *cenocepacia* sensor kinase hybrid AtsR is a global regulator modulating quorum-sensing
718 signalling. Environ Microbiol 15:372–385.

719 54. Henry DA, Campbell ME, LiPuma JJ, Speert DP. 1997. Identification of *Burkholderia*
720 *cepacia* isolates from patients with cystic fibrosis and use of a simple new selective
721 medium. J Clin Microbiol 35:614–619.

722 55. Schneider CA, Rasband WS, Eliceiri KW. 2012. NIH Image to ImageJ: 25 years of image
723 analysis. Nat Methods 9:671–675.

724 56. Christensen QH, Grove TL, Booker SJ, Greenberg EP. 2013. A high-throughput screen for
725 quorum-sensing inhibitors that target acyl-homoserine lactone synthases. Proc Natl Acad
726 Sci U S A 110:13815–13820.

727 57. McInnis CE, Blackwell HE. 2011. Thiolactone modulators of quorum sensing revealed
728 through library design and screening. Bioorg Med Chem 19:4820–4828.

729 58. O'Grady EP, Viteri DF, Sokol PA. 2012. A unique regulator contributes to quorum sensing
730 and virulence in *Burkholderia cenocepacia*. PloS One 7:e37611.

731 59. Chapalain A, Vial L, Laprade N, Dekimpe V, Perreault J, Déziel E. 2013. Identification of
732 quorum sensing-controlled genes in *Burkholderia ambifaria*. MicrobiologyOpen 2:226–
733 242.

734 60. Uzelac G, Patel HK, Devescovi G, Licastro D, Venturi V. 2017. Quorum sensing and RsaM
735 regulons of the rice pathogen *Pseudomonas fuscovaginae*. Microbiol Read Engl.

736 61. Livak KJ, Schmittgen TD. 2001. Analysis of relative gene expression data using real-time
737 quantitative PCR and the 2(-Delta Delta C(T)) Method. Methods San Diego Calif 25:402–
738 408.

739 62. Schmittgen TD, Livak KJ. 2008. Analyzing real-time PCR data by the comparative C(T)
740 method. Nat Protoc 3:1101–1108.

741 63. Peeters E, Sass A, Mahenthiralingam E, Nelis H, Coenye T. 2010. Transcriptional response
742 of *Burkholderia cenocepacia* J2315 sessile cells to treatments with high doses of hydrogen
743 peroxide and sodium hypochlorite. BMC Genomics 11:90.

744 64. Wong Y-C, Abd El Ghany M, Ghazzali RNM, Yap S-J, Hoh C-C, Pain A, Nathan S. 2018.
745 Genetic Determinants Associated With *in vivo* Survival of *Burkholderia cenocepacia* in the
746 *Caenorhabditis elegans* Model. Front Microbiol 9:1118.

747 65. Chapalain A, Groleau M-C, Le Guillouzer S, Miomandre A, Vial L, Milot S, Déziel E.
748 2017. Interplay between 4-Hydroxy-3-Methyl-2-Alkylquinoline and N-Acyl-Homoserine
749 Lactone Signaling in a *Burkholderia cepacia* Complex Clinical Strain. Front Microbiol
750 8:1021.

751

752

753 **Table 1: CepI activity is not inhibited by the presence of PAA or PAA-CoA.**

Conditions	Enzyme activity ± SD (min^{-1})
C8-ACP + SAM	3.46 ± 0.12
C8-ACP + SAM + 200 µM PAA	3.29 ± 0.21
C8-ACP + SAM + 200 µM PAA-CoA	3.04 ± 0.29

754

755 **Table 2. Bacterial strains used in this study.**

Strains	**Features**	**Reference or source**
Burkholderia cenocepacia		
K56-2 (LMG18863)	WT strain, ET12 clone related to a cystic fibrosis clinical isolate, J2315	(43)
ΔpaaABCDE	Deletion of *paaABCDE* operon in K56-2	(18)
ΔpaaK1	Deletion of *paaK* gene on chromosome 1 (BCAL0404) in K56-2	This study
ΔpaaK2	Deletion of *paaK* gene on chromosome 2 (BCAM1711) in K56-2	This study
ΔpaaK1Δpaak2	Deletion of *paaK* gene on chromosome 2 (BCAM1711) in K56-2*ΔpaaK1*	This study
ΔpaaK2Δpaak1	Deletion of *paaK* gene on chromosome 1 (BCAL0404) in K56-2*ΔpaaK2*	This study
ΔcepI	Deletion of BCAM1870 in K56-2	This study
ΔcepR	Deletion of BCAM1868 in K56-2	This study
ΔpaaABCDEΔcepI	Deletion of BCAM1870 in K56-2*ΔpaaABCDE*	This study
ΔpaaABCDEΔcepR	Deletion of BCAM1868 in K56-2*ΔpaaABCDE*	This study
ΔpaaK1ΔpaaK2ΔcepI	Deletion of BCAM1870 in K56-2*ΔpaaK1ΔpaaK2*	This study
ΔpaaK1ΔpaaK2ΔcepR	Deletion of BCAM1868 in K56-2*ΔpaaK1ΔpaaK2*	This study

ΔpaaK2ΔpaaK1ΔcepI	Deletion of BCAM1870 in K56-2*ΔpaaK2ΔpaaK1*	This study
ΔpaaK2ΔpaaK1ΔcepR	Deletion of BCAM1868 in K56-2*ΔpaaK2ΔpaaK1*	This study
Escherichia coli		
OP50	Uracil auxotroph	*Caenorhabditis* Genetic Center (University of Minnesota, Minneapolis, USA)
MM290		
SY327lpir	*araD Δ(lac pro) argE*(Am) *recA56 rifR nalA λpir*	(44)
W14	*E. coli* W with deletion encompassing PAA pathway genes.	(45, 46)

Table 3. Plasmids used in this study.

Plasmids	Features	Reference or source
pRK2013	ori_{colE1}, RK2 derivative, Kan^R, mob^+, tra^+	(47)
pGPI-*Sce*I	ori_{R6K}, I-*Sce*I recognition sequence, Tmp^R	(48)
pDAI-*Sce*I	DHFR promoter controlling e-I-*Sce*I, Tet^R	(48)
pBAD30	ori_{p15A} *araC* P_{BAD} Amp^R	(49)
pTL5	pBAD30 containing CepR (BCAM1868) with Shine Dalgarno region	This study
pBBR*lux*	*luxCDABE*-based promoter plasmid	(50)
pTL7	pBBR*lux* containing *cepI* promoter region (upstream of BCAM1870)	This study
pTL12	pBBR*lux* containing *araC* and P_{BAD} promoter	This study
pTL13	pBBR*lux* containing *dhfr* promoter region	This study

pTL17	pGPI-SceI containing custom gene fragment for the deletion of *paaK1* (BCAL0404) in K56-2	This study
pTL18	pGPI-SceI containing custom gene fragment for the deletion of *paaK2* (BCAM1711) in K56-2	This study
pTnMod-STp	*ori_{pSC101} Tn5 inverted repeats Tn5 transposase Tmp^R*	(51)
pTL9	*BglII restriction digest of pTnMod-STp to remove Tn5 transposase*	This study
pTL21	*ori_{pSC101} rhaR rhaS P_{rhaB} Tmp^R*	This study
pTL22	*pTL21 expressing rhamnose-inducible paaK (ECW_m1532)*	This study
pAAD	*15.4 Kb region contains paa cluster from E. coli W*	(46)
pSCrhaB2	*ori_{pBBR1} rhaR rhaS P_{rhaB}* Tmp^R *mob^+*	(52)
pKF2	pSCrhaB2 expressing rhamnose-inducible *paaK2* (BCAM1711)	This study
pCP300	*cepI::luxCDABE* transcriptional promoter fusion in pMS402	(53)
pPromcepR	*cepR::luxCDABE* transcriptional promoter fusion in pMS402	(53)
pMS402	*luxCDABE*-based promoter reporter plasmid, Kan^R Tp^R	(53)
pDelCepR	pGPI-*Sce*I containing the upstream and downstream regions of *cepR* for marker-less deletion in K56-2	(53)
pDelCepI	pGPI-*Sce*I containing the upstream and downstream regions of *cepR* for marker-less deletion	(53)

758 Amp^R, Ampicillin resistance; Kan^R, Kanamycin resistance; Tmp^R, Trimethoprim resistance;

759 Tet^R, Tetracycline resistance.

760

761 **Table 4. Primers used in this study.** Restriction sites are underlined and start or stop codons are
762 in bold.
763

Primer #	Sequence (5'-3')	Restriction site	Template and location
900	TGCAACTCGTACAACCT	n/a	K56-2 upstream of BCAL0404
901	CCTGTGATTTAGGTTCGC	n/a	K56-2 downstream of BCAL0404
902	AAGGGCGTGAACTATCC	n/a	K56-2 upstream of BCAM1711
903	TAGAACGGCACACCTC	n/a	K56-2 downstream of BCAM1711
980	GTTGACATGACGAACGCCAC	n/a	K56-2 upstream of BCAL0404
981	GACATGCCGACCAAGGAAGA	n/a	K56-2 downstream of BCAL0404
982	CCGTTCGAGTTGATGGACCT	n/a	K56-2 upstream of BCAM1711
983	CGCATCGAAAAAGCGCTTGA	n/a	K56-2 downstream of BCAM1711
1055	GTGACTCAT**ATG**ACTCACCCGACGCATC	*Nde*I	K56-2 BCAM1711
1056	TTGACTTCTAGACTTCAATTCACCCATCGAACAG	*Xba*I	K56-2 downstream of BCAM1711
848	CCGCCAGGCAAATTCTGTTT	n/a	pSCrhaB2 downstream of the MCS
920	GCTTTCTGATAGTTGTTGTGG	n/a	pDAI-*Sce*I
921	AGGTTGTTCGGGATGG	n/a	pDAI-*SceI*

154	ACAGGAACACTTAACGGCTGACATG	n/a	External to the MCS on pGPI-*Sce*I
1080	GACAAGGGTTCGATCCAG	n/a	pDelCepR
1081	GATGGCCATCACGTTGCT	n/a	pDelCepR
1082	CATGACTTCACCCTTGC	n/a	pDelCepI
1083	CTTCGATGAACTGCGC	n/a	pDelCepI
1112	GTTGGTAGGCATCCTGC	n/a	K56-2 upstream of BCAM1870
1113	GTCGGTCAATGCGTGTC	n/a	K56-2 downstream of BCAM1870
703	ATTAGAGAATTCGGAGAAAGAATGGAACTGCGC	*Eco*RI	K56-2 BCAM1868
704	TCTAATTCTAGATCAGGGTGCTTCGATGAGC	*Xba*I	K56-2 BCAM1868
712	TCTAATACTAGTTGGCGCTCTTTATAAGC	*Spe*I	K56-2 BCAM1870 promoter region
713	TTGATCGGATCC**TCA**GAGTTCGTGTGGCAACC	*Bam*HI	K56-2 BCAM1870 promoter region
768	AAGTATGAGCTCCAAGCCGTCAATTGTC	*Sac*I	pBAD30 P_{BAD} region
769	TAAGATACTAGTAACAGTAGAGAGTTGCG	*Spe*I	pBAD30 P_{BAD} region
770	AAGTATGAGCTCGACATAAGCCTGTTCGG	*Sac*I	pTnMod-STp P_{DHFR} region
771	TAAGATACTAGTTCAGTTGGCTTCATCGCTAC	*Spe*I	pTnMod-STp P_{DHFR} region
750	TACGCCGAAATCAACGACCA	n/a	qPCR primer for BCAM0918 (*rpoD*)
751	ACTTCGGCTTCCTCTTCGAC	n/a	qPCR primer for

			BCAM0918 (*rpoD*)
1033	AAGTTTCGAGCGTGACCAGTTC	n/a	qPCR primer for BCAM1870 (*cepI*)
1034	AACAGCGACTTCAGCAGATACG	n/a	qPCR primer for BCAM1870 (*cepI*)
1035	CGGATTCGAATACTGCTGTTACGG	n/a	qPCR primer for BCAM1868 (*cepR*)
1036	CTCGATGTAGTTCTGCGCCTG	n/a	qPCR primer for BCAM1868 (*cepR*)

764

765

766

767 **Figure Legends**

768 **Fig. 1: The proposed phenylacetic acid degradation (PAA) pathway in *B. cenocepacia.***
769 Based on the pathway described in *E. coli* and *Pseudomonas* by Teufel *et al.* (2010),
770 phenylalanine (Phe) is degraded to PAA and the first step of the pathway is the conversion of
771 PAA to phenylacetyl-CoA (PAA-CoA) by the phenylacetyl-CoA ligase, **PaaK** (shown in
772 purple). The phenylacetyl-CoA thioesterase, **PaaI,** can reversibly convert PAA-CoA back to
773 PAA to prevent toxic accumulation of the epoxide if the downstream pathway is blocked. PAA-
774 CoA is epoxidized by the ring 1,2 phenylacetyl-CoA epoxidase, **PaaABCDE** (shown in orange),
775 forming ring-1,2-epoxyphenylacetyl-CoA or epoxide (EP-CoA). The epoxide is further degraded
776 to components of the TCA cycle, acetyl-CoA and succinyl-CoA.

777

778 **Fig. 2: Characterization of the growth and metabolite production of *B. cenocepacia***
779 **PAA pathway mutants. A)** Growth curves of *B. cenocepacia* K56-2 PAA pathway mutants on
780 LB media. **B)** Endpoint growth of *B. cenocepacia* K56-2 PAA pathway mutants. Strains were
781 cultured on M9 with 25 mM Glucose or with 5 mM PAA as the sole carbon sources for 48 hours
782 and the OD_{600} was measured. Error bars represent SD for three biological replicates. a represents
783 no significant difference, b represents p values ≤ 0.05 as determined by student's T-test (two
784 tailed) when compared to growth on PAA of K56-2. **C-F)** Cultures were grown to late
785 exponential phase and equal volumes of whole-cell cultures and filtered supernatants were
786 frozen, extracted with 75% (v/v) ethanol and analyzed with ion pair reversed phase ultra-high
787 performance liquid chromatography tandem mass spectrometry (IP-RP-UHPLC-MS/MS).
788 Extracellular and intracellular levels of PAA (**C-D)** and PAA-CoA (**E-F**). A horizontal line
789 represents the mean and an asterix denotes $p \leq 0.05$ as determined by student's T-test (two

790 tailed) when compared to K56-2 (**C**) or Δ*paaABCDE* (**F**). The limits of detection for PAA (1μM)
791 and PAA-CoA (0.3 μM) are indicted by red lines. Two biological replicates with three technical
792 replicates each were performed.
793
794 **Fig. 3: The Δ*paaK1*Δ*paaK2* mutant is more virulent than wild type in *C. elegans* and has**
795 **higher proteolytic activity. A)** Slow killing assays with *C. elegans* over a period of seven days
796 show that the Δ*paaK1*Δ*paaK2* mutant kills *C. elegans* in a similar time frame as wild type,
797 whereas the nematodes exposed to the Δ*paaABCDE* mutant have increased survival (n = ~70-
798 100 nematodes per strain). The increased killing ability of the Δ*paaK1*Δ*paaK2* mutant compared
799 to wild type was determined as significant according to the log-rank test ($p < 0.001$). Three
800 biological replicates were performed. **B)** Proteolytic activity was measured as the area of the
801 zone of clearance (excluding colonies) on agar containing 2% skim milk with or without the
802 addition of 2 mM of phenylalanine. The error bars represent the SD of three independent
803 experiments. An asterix '*' denotes significant difference from wild type ($p < 0.05$) and '**'
804 denotes significant difference from wild type ($p < 0.01$).
805
806 **Fig. 4: Neither PAA nor PAA-CoA affect the formation of CepR:C8-HSL complexes. A)**
807 The CepR reporter strain and control strains used. Regulatory genes *araC* (for P_{BAD}) and *rhaSR*
808 (for P_{rhaBAD}) were excluded from the figure for simplicity. **B)** In the presence of 0.01% rhamnose
809 (rha), 0.5 mM of PAA was converted to PAA-CoA by the PaaK ligase in the CepR reporter
810 strain. For the reporter system 0.2% arabinose was used to induce the expression of *cepR* and the
811 calculated EC_{50} of C8-HSL (20 nm) was used to activate the system. **C)** To test the effect of
812 PAA-CoA, 0.5 mM PAA and 0.01% rhamnose were added and the % activity (activity in the

813 presence of rhamnose compared to in the absence of rhamnose) was determined at 3 hours. PAA-
814 CoA had no effect on the CepR reporter strain compared to that of the effect on control strains.
815 **D)** PAA itself was tested at various concentrations from 0.1-1 mM (0.1 mM shown here) and
816 percent activity was calculated for the presence of PAA compared to the absence of PAA at 2
817 hours. No effect was observed when compared to the control strains. The error bars represent the
818 SD of three independent experiments.
819
820 **Fig. 5: Transcription of *cepI* and *cepR* and C8-HSL production is not decreased in any of**
821 **the PAA pathway mutants. A)** RT-qPCR shows that *cepI* and *cepR* gene expression is not
822 decreased compared to wild type in the PAA pathway mutants. **B)** C8-HSL levels were not
823 decreased in any of the mutants, but C8-HSL levels were higher in the Δ*paaABCDE* mutant.
824 Virulence of strains in both *C. elegans* assays and exoprotease activity assays is denoted above
825 the graphs per the results from Fig. 3.
826
827 **Fig. 6: The virulence of Δ*paaK1*Δ*paaK2*Δ*cepR* is independent of the CepIR QS system. A)**
828 The *cepI* and *cepR* mutations in a Δ*paaK1*Δ*paaK2* mutant have opposing levels of virulence.
829 Δ*paaK1*Δ*paaK2*Δ*cepR* is as virulent as wild type whereas Δ*paaK1*Δ*paaK2*Δ*cepI* is attenuated for
830 virulence in *C. elegans*. **B)** *cepI* and *cepR* mutants have similar levels of attenuation in *C.*
831 *elegans*. Figures **A)** and **B)** are representative of three biological replicates (n = ~70 - 110
832 nematodes per strain). **C)** The Δ*paaK1*Δ*paaK2*Δ*cepR* mutant has wild type levels of proteolytic
833 activity with or without phenylalanine whereas the Δ*cepR* mutant has decreased proteolytic
834 activity. Proteolytic activity was measured as the area of the zone of clearance (excluding
835 colonies) on agar containing 2% skim milk with or without the addition of 2 mM of

836 phenylalanine. **D)** *cepR* transcription is restored to wild type levels in Δ*paaABCDE*Δ*cepI* and
837 Δ*paaK1*Δ*paaK2*Δ*cepI* indicating that PAA restores *cepR* transcription. **E)** *cepI* is downregulated
838 in all of the Δ*cepR* mutants. **F)** C8-HSL levels were measured and none of the QS mutants had
839 detectable levels of C8-HSL. The error bars represent the SD of three independent experiments.
840
841 **Supplemental Material Figure Legends**
842 (see Supplemental Material document for Tables and Figures)
843
844 **Table S1. Gene fragment sequences flanking the regions of target genes.**
845
846 **Fig. S1: 0.02 µM (20 nM) is the effective concentration (EC_{50}) of C8-HSL with the CepR**
847 **reporter system.** The CepR reporter system was tested with varying concentrations of *N*-
848 octanoyl homoserine lactone (C8-HSL) to determine the concentration required for half maximal
849 signal. The signal was measured over 4 hours and the time point where the signal was highest (2
850 hours) was used. Data was graphed and the EC_{50} was calculated using GraphPad Prism. Error
851 bars are standard deviations of two replicates. For the conditions of this reporter system the EC_{50}
852 of C8-HSL is 20 nM.
853
854 **Fig. S2: Growth of *paaK* ligase mutants on M9 with 5 mM PAA was restored by pKF2, a**
855 **rhamnose-inducible *paaK* ligase expression vector.** *B. cenocepacia* strains were grown on M9
856 with 25 mM of glucose or 5 mM of PAA as a sole carbon source. There was no difference of
857 growth of *B. cenocepacia* K56-2 containing the empty vector (pSCrhaB2) in the presence of
858 0.01% (v/v) rhamnose on glucose or PAA as a sole carbon source. When the *paaK* ligase

859 expression vector (pKF2) was induced with rhamnose in the K56-2*ΔpaaK1ΔpaaK2* and the K56-
860 2*ΔpaaK2ΔpaaK1* strains growth was restored on PAA. This was not the case for the empty
861 vector controls, indicating that the PAA pathway interruption in this mutant can be
862 complemented with the introduction of BCAM1711 (*paaK2*) in trans. Error bars represent
863 standard deviations of three biological replicates.
864
865 **Fig. S3: *C. elegans* slow killing assays show that the *paaK* single deletion mutants have wild**
866 **type levels of virulence but the double *paaK* knockout mutants have increased virulence**
867 **compared to wild type. A)** *ΔpaaK2ΔpaaK1* had slightly increased virulence compared to wild
868 type as determined by the log-rank test ($p < 0.001$). **B)** The *ΔpaaK1* and *ΔpaaK2* single deletion
869 mutants have wild type levels virulence in a *C. elegans* model of infection. This figure is
870 representative of at least three independent experiments. **C)** Proteolytic activity was measured as
871 the area of the zone of clearance (excluding colonies) on agar containing 2% skim milk with or
872 without the addition of 2 mM of phenylalanine. The error bars represent the SD of three
873 independent experiments. An asterix '*' denotes significant difference from wild type ($p < 0.05$)
874 and '**' denotes significant difference from wild type ($p < 0.01$).
875
876 **Fig. S4: The concentration of extracellular PAA does not correlate with the virulence of**
877 **PAA pathway mutants**. Correlation between the extracellular concentration of PAA (μM) and
878 the A) median survival of *C. elegans* ($p = 0.148$) in slow killing assays or B) proteolytic activity
879 on 2% skim milk agar supplemented with 2 mM phenylalanine ($p = 0.114$).
880

881 **Fig. S5: Transcription of *cepI* and *cepR* and C8-HSL production is not decreased in any of**
882 **the PAA pathway mutants. A)** RT-qPCR shows that *cepI* and *cepR* gene expression is not
883 decreased compared to wild type in the PAA pathway mutants. Error bars are standard deviations
884 of three biological replicates. **B)** C8-HSL levels were not decreased in any of the mutants, but
885 C8-HSL levels were higher in the Δ*paaABCDE* and Δ*paaK2*Δ*paaK1* mutants. The bar is the
886 mean of three biological replicates. Virulence is for *C. elegans* slow killing assays and
887 exoprotease assays as seen in Fig. 3.
888
889 **Fig. S6: Mutations of *cepI* and *cepR* in the PAA pathway mutant backgrounds result in no**
890 **visible growth defects.** Mutants were grown in LB from a starting OD_{600} of 0.04 over 24 hours
891 and showed no significant growth defects compared to wild type. Error bars are standard
892 deviation of three biological replicates.
893
894 **Fig. S7: The virulence of Δ*paaK2*Δ*paaK1*Δ*cepR* is independent of the CepIR QS system. A)**
895 *cepI* and *cepR* deletions in wild type and Δ*paaABCDE* mutant backgrounds led to attenuation of
896 virulence in *C. elegans*. The Δ*paaABCDE* mutant is attenuated compared to wild type but is less
897 attenuated than *cepI* and *cepR* mutants. **B)** As seen with the Δ*paaK1*Δ*paaK2*Δ*cepR* mutant, the
898 *paaK2*Δ*paaK1*Δ*cepR* mutant displays CepR-independent virulence in *C. elegans*. A *cepI* deletion
899 in the Δ*paaK2*Δ*paaK1* mutant resulted in similar attenuation to that of the *cepI* and *cepR*
900 deletions in wild type backgrounds. **C)** The Δ*paaK2*Δ*paaK1*Δ*cepR* mutant has wild type levels
901 of exoprotease activity with or without phenylalanine whereas the Δ*cepR* mutant has decreased
902 exoprotease activity. Exoprotease activity was measured as the area of the zone of clearance
903 (excluding colonies) on agar containing 2% skim milk with or without the addition of 2 mM of

904 phenylalanine. **D)** *cepR* transcription is restored to wild type levels in Δ*paaABCDE*Δ*cepI* and
905 Δ*paaK2*Δ*paaK1*Δ*cepI* indicating that PAA increases *cepR* transcription. **E)** *cepI* is
906 downregulated in all of the Δ*cepR* mutants. **F)** C8-HSL levels were measured and none of the QS
907 mutants had detectable levels of C8-HSL. Experiments were performed in triplicate. The error
908 bars represent the SD of three independent experiments.
909

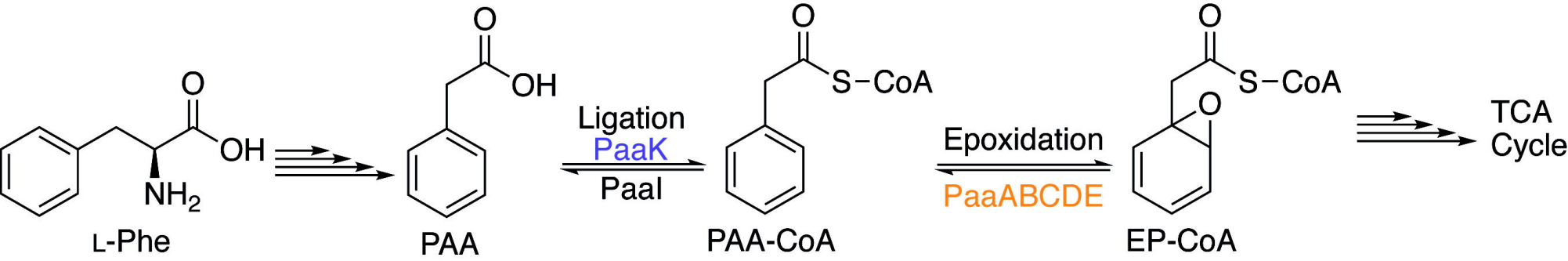
O
OH
NH2
L-Phe
O
OH
PAA
Ligation
PaaK
PaaI
O
S−CoA
PAA-CoA
Epoxidation
PaaABCDE
O
S−CoA
O
EP-CoA
TCA
Cycle

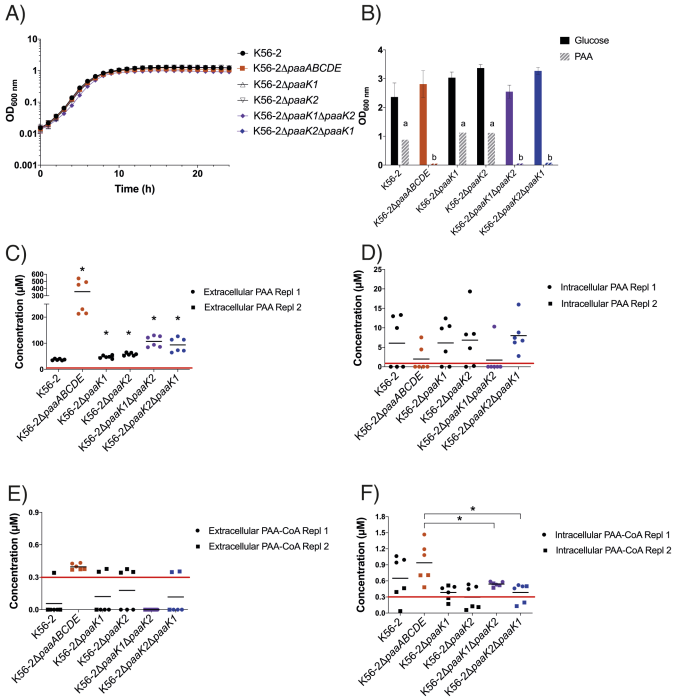
A)
B)
C)
D)
E)
F)
K56-2
K56-2ΔpaaABCDE
K56-2ΔpaaK1
K56-2ΔpaaK2
K56-2ΔpaaK1ΔpaaK2
K56-2ΔpaaK2ΔpaaK1
OD600 nm
Time (h)
Glucose
PAA
Concentration (μM)
Extracellular PAA Repl 1
Extracellular PAA Repl 2
Intracellular PAA Repl 1
Intracellular PAA Repl 2
Extracellular PAA-CoA Repl 1
Extracellular PAA-CoA Repl 2
Intracellular PAA-CoA Repl 1
Intracellular PAA-CoA Repl 2

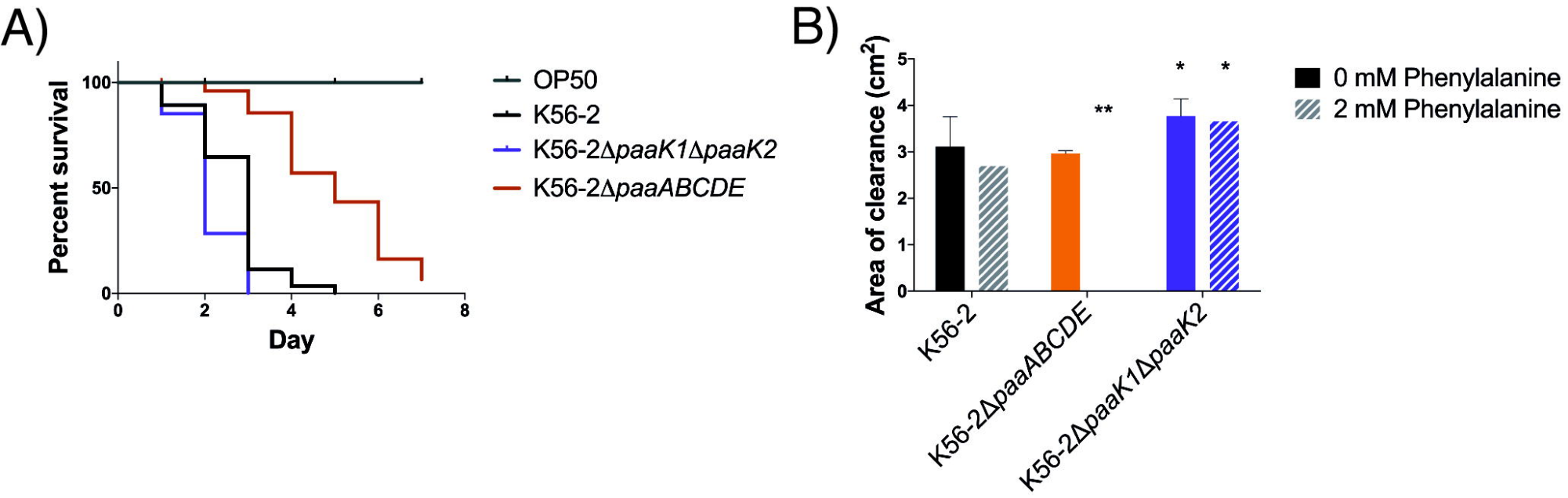
A)
Percent survival
100
50
0
0
2
4
6
8
Day
OP50
K56-2
K56-2ΔpaaK1ΔpaaK2
K56-2ΔpaaABCDE
B)
Area of clearance (cm2)
5
4
3
2
1
0
**
*
*
K56-2
K56-2ΔpaaABCDE
K56-2ΔpaaK1ΔpaaK2
0 mM Phenylalanine
2 mM Phenylalanine

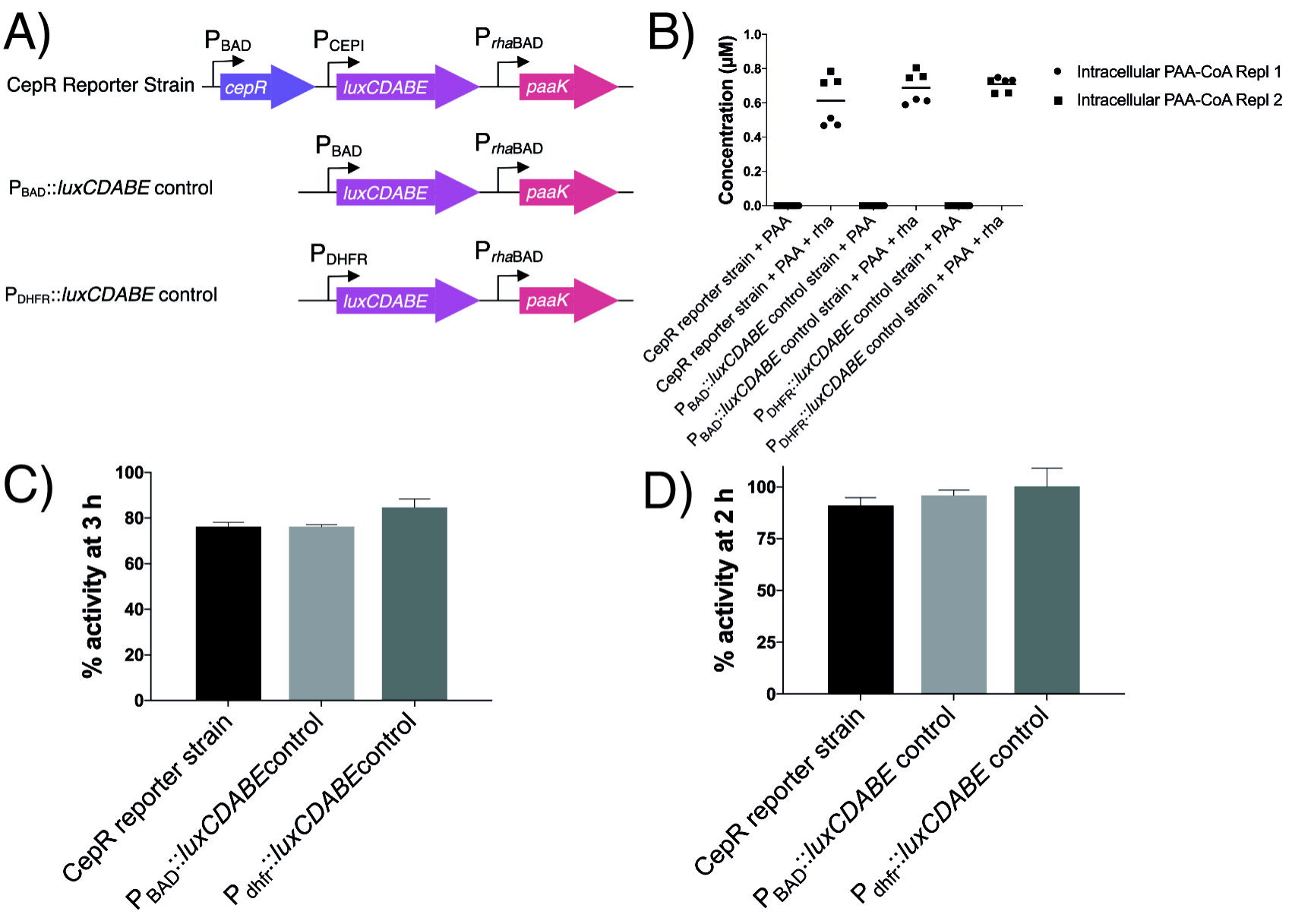
A)
CepR Reporter Strain
P_{BAD}
P_{CEPI}
P_{rhaBAD}
cepR
luxCDABE
paaK
P_{BAD}::luxCDABE control
P_{BAD}
P_{rhaBAD}
luxCDABE
paaK
P_{DHFR}::luxCDABE control
P_{DHFR}
P_{rhaBAD}
luxCDABE
paaK
B)
Concentration (μM)
1.0
0.8
0.6
0.4
0.2
0.0
Intracellular PAA-CoA Repl 1
Intracellular PAA-CoA Repl 2
CepR reporter strain + PAA
CepR reporter strain + PAA + rha
P_{BAD}::luxCDABE control strain + PAA
P_{BAD}::luxCDABE control strain + PAA + rha
P_{DHFR}::luxCDABE control strain + PAA
P_{DHFR}::luxCDABE control strain + PAA + rha
C)
% activity at 3 h
100
80
60
40
20
0
CepR reporter strain
P_{BAD}::luxCDABEcontrol
P_{dhfr}::luxCDABEcontrol
D)
% activity at 2 h
100
75
50
25
0
CepR reporter strain
P_{BAD}::luxCDABE control
P_{dhfr}::luxCDABE control

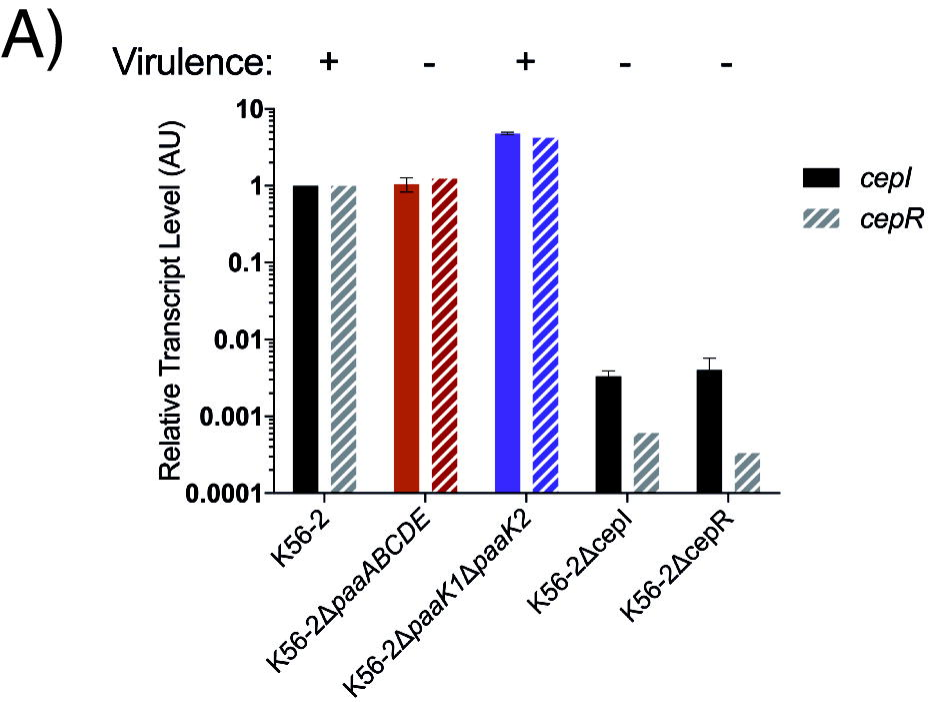
A)
Virulence: + - + - -
Relative Transcript Level (AU)
10
1
0.1
0.01
0.001
0.0001
cepI
cepR
K56-2
K56-2ΔpaaABCDE
K56-2ΔpaaK1ΔpaaK2
K56-2ΔcepI
K56-2ΔcepR

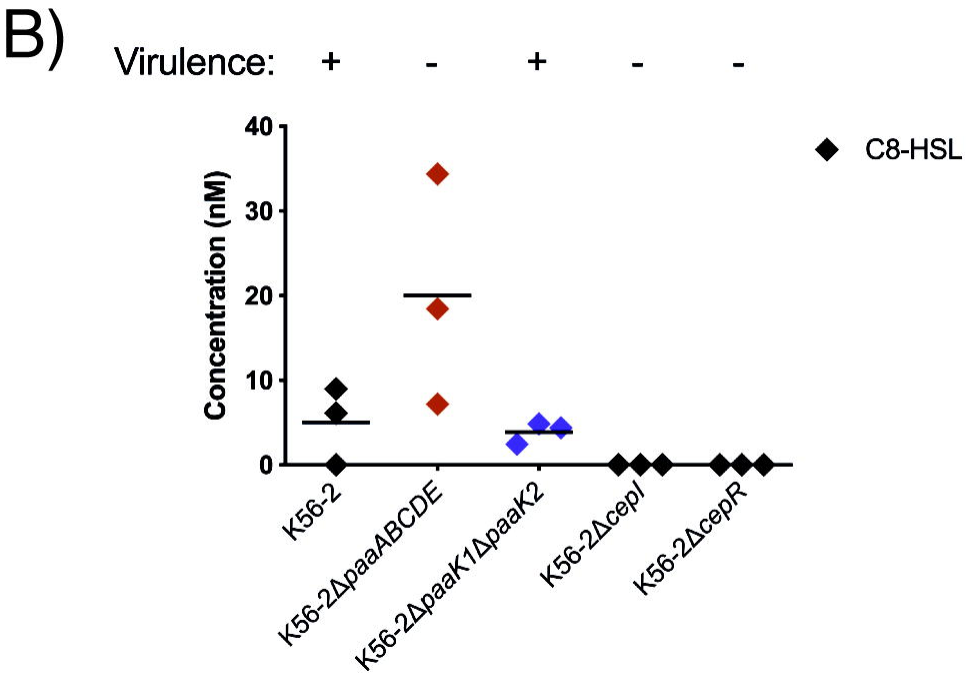
B)
Virulence: + - + - -
Concentration (nM)
40
30
20
10
0
C8-HSL
K56-2
K56-2ΔpaaABCDE
K56-2ΔpaaK1ΔpaaK2
K56-2ΔcepI
K56-2ΔcepR

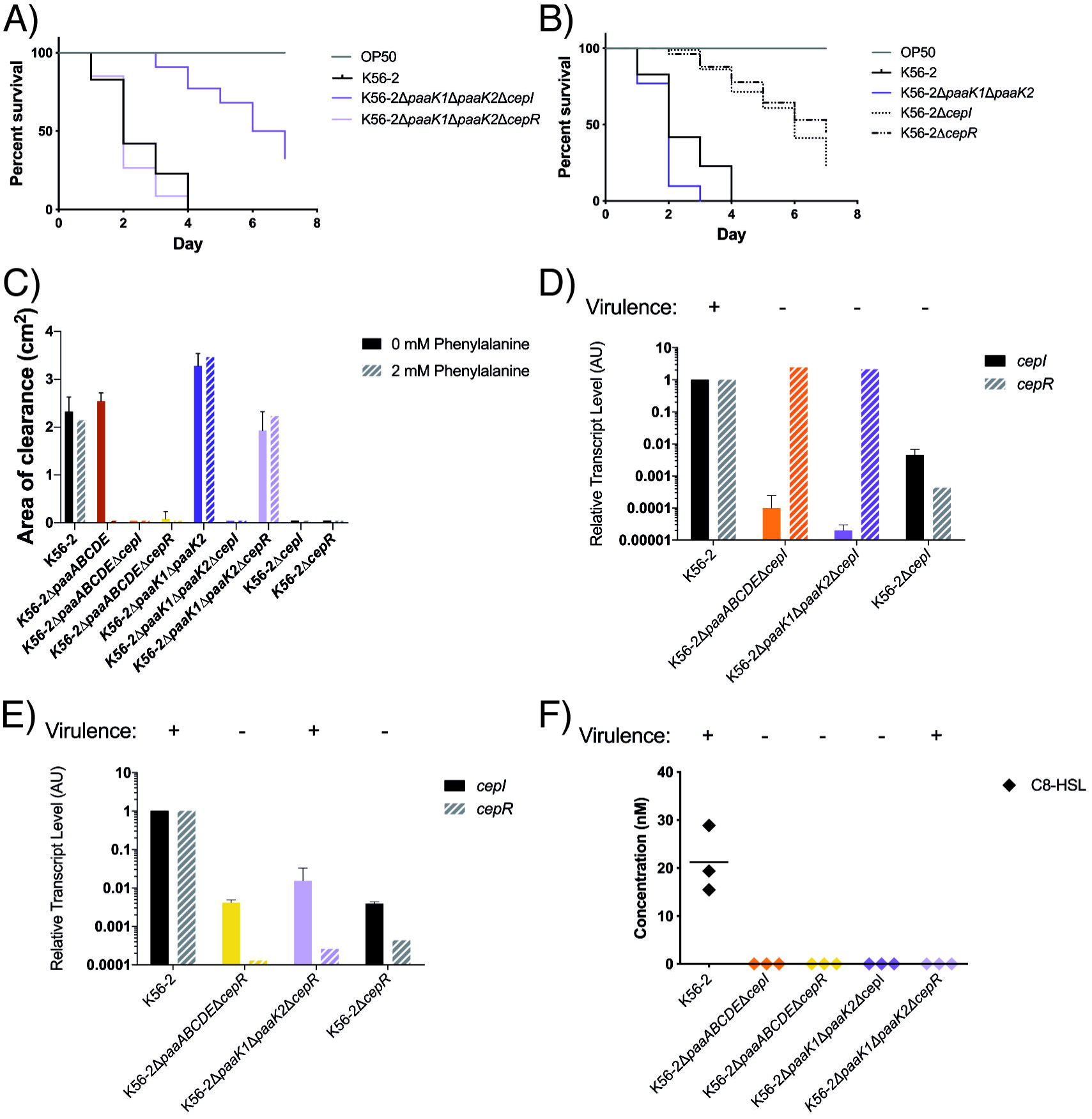
A)
Percent survival
Day
OP50
K56-2
K56-2ΔpaaK1ΔpaaK2ΔcepI
K56-2ΔpaaK1ΔpaaK2ΔcepR
B)
Percent survival
Day
OP50
K56-2
K56-2ΔpaaK1ΔpaaK2
K56-2ΔcepI
K56-2ΔcepR
C)
Area of clearance (cm²)
0 mM Phenylalanine
2 mM Phenylalanine
K56-2
K56-2ΔpaaABCDE
K56-2ΔpaaABCDEΔcepI
K56-2ΔpaaABCDEΔcepR
K56-2ΔpaaK1ΔpaaK2
K56-2ΔpaaK1ΔpaaK2ΔcepI
K56-2ΔpaaK1ΔpaaK2ΔcepR
K56-2ΔcepI
K56-2ΔcepR
D)
Virulence: + - - -
Relative Transcript Level (AU)
cepI
cepR
K56-2
K56-2ΔpaaABCDEΔcepI
K56-2ΔpaaK1ΔpaaK2ΔcepI
K56-2ΔcepI
E)
Virulence: + - + -
Relative Transcript Level (AU)
cepI
cepR
K56-2
K56-2ΔpaaABCDEΔcepR
K56-2ΔpaaK1ΔpaaK2ΔcepR
K56-2ΔcepR
F)
Virulence: + - - - +
Concentration (nM)
C8-HSL
K56-2
K56-2ΔpaaABCDEΔcepI
K56-2ΔpaaABCDEΔcepR
K56-2ΔpaaK1ΔpaaK2ΔcepI
K56-2ΔpaaK1ΔpaaK2ΔcepR